Atmospheric Pollution Research 15 (2024) 102244

Contents lists available at ScienceDirect

Atmospheric Pollution Research

journal homepage: www.elsevier.com/locate/apr

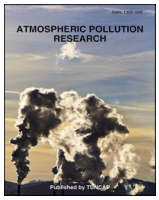

Interannual and spatial variations in acid-soluble trace elements in snow: comparison with the mineralogy of dusts from open pit bitumen mining

Fiorella Barraza, Andreas Hamann, Tommy Noernberg, Judy Schultz, William Shotyk *

Department of Renewable Resources, University of Alberta Edmonton, AB, Canada

ARTICLE INFO

Keywords:
Trace elements
Acid solubility
Snow
Dusts
ABS region

ABSTRACT

There is ongoing concern about trace element (TE) emissions to the global environment from the dusts generated by open pit mining of coal, iron ore, stone quarries, and aggregate extraction. However, the chemical composition and acid solubility of these dusts is highly variable. Here, TEs were determined in snow collected in 2016 and 2017 in the vicinity of open-pit bitumen mines in northern Alberta, Canada. Acid solubility was assessed quantitatively by comparing TE concentrations in leachates and acid digests. The mineralogical composition of the particles extracted from the snow was examined using SEM-EDS. The data is reproducible from one year to the next. TE concentrations were greater throughout the industrial zone compared to the reference location (UTK), with the midpoint between the two central upgraders being especially impacted. Regardless of their geochemical class (lithophile: Al, Be, Cs, La, Li, Sr, Th; chalcophile: As, Cd, Pb, Sb, Tl; or enriched in bitumen: Mo, Ni, V), all TEs showed strong, positive correlations with Y, a conservative element which serves as a surrogate for the abundance of mineral particles. The ratio V:Ni in the snow is less than the corresponding values for bitumen and petcoke, but similar to that of local road dust. The ratio La:Al in snow is elevated, relative to the earth's crust, suggesting an enrichment of heavy minerals monazite and zircon. The predominance of quartz and other stable silicates helps to explain the limited chemical solubility of the dusts, and predicts a low bioaccessibility of these TEs in the environment.

1. Introduction

Atmospheric dust particles, which can contain trace elements (TEs), are known to have an impact on the environment and human health (Field et al., 2010; Luo et al., 2019; Morman and Plumlee, 2013; Schepanski, 2018; Scheuvens and Kandler, 2014; Simonson, 1995; Vithanage et al., 2022). These particles are removed from the atmosphere by dry and wet deposition (Bergametti and Forêt, 2014; Rodríguez et al., 2012; Seinfeld and Pandis, 2016; Vithanage et al., 2022), which are key processes controlling their lifetime and therefore determine their potential biogeochemical impact (Adebiyi et al., 2023; Bergametti and Forêt, 2014; Cheng et al., 2021). Sources of atmospheric particulate matter in the environment can be natural (e.g volcanic eruptions, soil erosion) and anthropogenic (e.g industrial activities, fossil fuel combustion) (Hopke et al., 2020; Luo et al., 2019; Scheuvens and Kandler, 2014; Vithanage et al., 2022).

The shape and size of dust particles are some of the main properties that govern their settling behavior and transport: coarse and larger particles (>10 μm) will deposit near the source of emission, whereas fine particles (<2 μm) will travel long distances (Adebiyi et al., 2023; Bergametti and Forêt, 2014; Schepanski, 2018; Scheuvens and Kandler, 2014; Seinfeld and Pandis, 2016). For example, orange-colored snow containing large dust particles (8–38 μm in diameter) was observed over the Pyrenees, French, and Swiss Alps during an extreme deposition event of Saharan dust (Dumont et al., 2023); brownish to black snow was reported in the remote Scottish Highlands due to long range transport of pulverized fuel and coal fly ash particles smaller than 4 μm (Davies et al., 1984); in New Zealand, fine atmospheric particles were likely due to wildfires in Australia (Pu et al., 2021); in the central Himalayas, dusts smaller than 2.5 μm were attributed to natural and anthropogenic sources (Svensson et al., 2021) and in northern Alberta, downwind from dry mine tailings, particles extracted from snow were in the size range of 10–100 μm (Javed et al., 2022).

When dust deposits on snow, the albedo is reduced, altering the

Peer review under responsibility of Turkish National Committee for Air Pollution Research and Control.

* Corresponding author. Bocock Chair for Agriculture and the Environment, 348B South Academic Building, Department of Renewable Resources, University of Alberta, Edmonton, AB, T6G 2G7, Canada.

E-mail addresses: barrazac@ualberta.ca (F. Barraza), shotyk@ualberta.ca (W. Shotyk).

https://doi.org/10.1016/j.apr.2024.102244
Received 22 February 2024; Received in revised form 5 June 2024; Accepted 30 June 2024
Available online 3 July 2024

melting behavior and the energy balance (Fassnacht et al., 2022; Field et al., 2010; Lehning, 2005; Pey et al., 2020; Reynolds et al., 2020; Schepanski, 2018; Tuzet et al., 2017; Warren, 2019). Moreover, several studies have reported an increase in the concentrations of major ions (Lawrence et al., 2010; Rhoades et al., 2010) and TEs (Carling et al., 2012; Pey et al., 2020) in snow associated with an increase of dust particles. During the initial snowmelt, ions are eluted from the snowpack at greater concentrations compared to the meltwater that is released afterwards (Colbeck, 1981; Davis, 1991; Feng et al., 2001; Hibberd, 1984; Johannessen and Henriksen, 1978; Lee and Jung, 2022). In some cases, the snowmelt runoff period accounts for a large percentage of the annual load of TEs to surface waters (Carling et al., 2015; Checketts et al., 2020; Rember and Trefry, 2004).

Not all of the TEs associated with dusts are in bioavailable form which is why it is fundamental to distinguish between the total and the «dissolved» (i.e. fraction that passes through a 0.45 μm filter) concentrations, the latter being the most relevant from the environmental and ecological point of view (Javed et al., 2022). From the legislative perspective, water quality guidelines - for human consumption and for the protection of aquatic life - are based on either total concentrations (CCME, 2023; Dunn et al., 2014; The European Comission, 2013) or on concentrations in the dissolved fraction (CCME, 2023; EPA, 2023). These guidelines constantly evolve to incorporate new findings about the bioaccumulation, bioavailability and toxicity of each targeted compound (Barnhart et al., 2021; Bogardi et al., 2020; Frisbie and Mitchell, 2022). From the analytical point of view, there are some challenges associated with the determination of TEs in snow such as sampling, handling and preparation especially for elements occurring at very low concentrations (Barbante et al., 2017; Boutron, 1990; Gabrielli et al., 2008; Javed et al., 2022; Krachler et al., 2005a). Regarding the methods to digest particulate matter in snow samples, HNO_3 is commonly used (Guéguen et al., 2016; Javed et al., 2022; Lai et al., 2017) to obtain « quasi-total » concentrations. Other authors propose a different approach and instead report the «acid-leachable» (or acid-soluble) fraction as way to characterize the reactivity of atmospheric particulate matter, and the relative solubility of TEs they contain (Koffman et al., 2014; Li et al., 2018; Spolaor et al., 2021).

Given that the dominant natural source of mineral dusts are small, soil and rock-derived particles (Kok et al., 2023; Shao, 2009), it is expected that some of these minerals are more soluble than others, releasing TEs at different rates and potentially resulting in a wide range of aqueous concentrations. For example, the lithophile elements such as Al and Si which dominate the primary silicate minerals (Goldschmidt, 1937) will be more resistant to acid-leaching than elements such as Ca, Mg and Sr which are abundant in carbonates and far more chemically reactive (Smrzka et al., 2019).

Open-pit bitumen mining in the Athabasca Bituminous Sands (ABS) region located in northern Alberta, Canada, generates large volumes of dusts not only from the extraction of this resource but also from road construction, unpaved roads, limestone quarries, overburden, coke piles, and dry tailings (Landis et al., 2017; Lynam et al., 2015; Mamun et al., 2021; Shotyk et al., 2016; Wang et al., 2015). Some studies in the ABS region have used snow to characterize the deposition of TEs and there is a common agreement that their concentrations increase with distance towards the centre of the industrial activities (Gopalapillai et al., 2019; Guéguen et al., 2016; Javed et al., 2017, 2022; Kelly et al., 2010; Kirk et al., 2018; Murray, 1981). Because dust deposition varies spatially and changes temporally, long-term monitoring is needed to assess the impact of such anthropogenic activities (Li et al., 2023; Wang et al., 2021). While the increase in total concentrations of dust particles and TEs toward industry is a legitimate concern, it is vital to understand the types of particles that host these elements, their mineralogical composition and acid solubility, and, ultimately, their potential to release TEs to the dissolved fraction of surface waters. To our knowledge there are no studies addressing these important details.

In our previous work (Barraza et al., 2024), we reported concentrations of 16 TEs obtained from melted and filtered snow (<0.45 μm), collected along the Athabasca River (AR), upstream and downstream of industry, in 2017. The acid-soluble fraction of TEs was used as a conservative estimate of the upper limit of the fraction that could potentially be mobilized under extremely acidic conditions (less than pH 1). However, a limited number of sampling locations was included in that report, and there was a single season of wintertime atmospheric deposition. In addition, mineralogical information about the particulate matter in the snow samples was limited.

To help fill these gaps and evaluate the reproducibility of the findings presented earlier, the aims of this study were to: (i) determine the interannual and spatial variations of TEs in the acid soluble fraction of snow collected in winter 2016 and 2017, (ii) quantify the extent of TE enrichments in snow collected near industry relative to UTK, the reference site, (iii) evaluate the consistency of the chemical behaviour of TEs in the dust particles between sampling years, and (iv) provide sufficient mineralogical information about the particulate fraction to help understand the limited bioaccessibility of the TEs, ; and v) to determine the possible ecological significance of TEs in snow relative to the dissolved fraction of the waters of the Athabasca River.

2. Materials and methods

2.1. Snow sampling and processing

The 2016 field campaign took place between February 24 and March 5 along the Athabasca River (AR) in the Athabasca Bituminous Sands (ABS) region, resulting in a collection of snow samples at 25 sites close to the east and west banks of the AR main stem (SAR) and at 5 tributary rivers (from the edge to 35 m into the river) (Fig. 1).

These samples complement the subsequent campaign during March 7 to 8, 2017 (Barraza et al., 2024). This transect covers approximately 120 km of the Lower AR watershed, and represents sites upstream, midstream and downstream of the industrial area (Table S1, Supplementary Information).

The weather conditions in the ABS region in 2016 were similar to those of 2017, with an average daily temperature ranging from −4.3 to −20.9 °C (slightly less cool than in 2017), although more warm days were recorded in 2016. The predominant wind directions in 2016 were ~18% from the south, 15% from the north and 15% from the southeast, similar to 2017 (~20% from the north and ~15% from the southeast %) (Fig. S1) (Government of Canada, 2022).

For comparison, snow was collected from the reference site Utikuma (UTK) during both years. The UTK site is an ombrotrophic peat bog located 264 km southwest from the ABS region (Fig. 1). The detailed justification for using this site as reference, was provided in the previous paper (Barraza et al., 2024).

The sampling procedure and preparation are described elsewhere (Barraza et al., 2024). In brief, snow samples were collected in triplicate in 1 L acid-cleaned polypropylene (PP) bottles from the top, middle, and bottom of the snowpack (from the top 5 cm to depths of 30–45 cm, depending on the accumulation of snow), as well as a bulk sample representing the entire snow profile. The acid-soluble fraction described hereafter refers to snow (collected in triplicate) that was melted, leached overnight with double-distilled nitric acid (final concentration of 0.5%), and filtered through an acid-cleaned 0.45 μm PTFE filter membrane. Additional information regarding the experimental methods used to validate the collection and handling of snow samples for the study of TEs is available in Javed et al. (2022). As in our previous study, the approach used to quantify the acid solubility of TEs was to calculate the percentage of each TE which is soluble in acid. This requires the determination of the «total » concentrations of TEs in bulk snow which is obtained after microwave digestion with concentrated HNO_3 (US EPA Methods 3050B and 3051A for TEs in soils) as described elsewhere (Barraza et al., 2024).

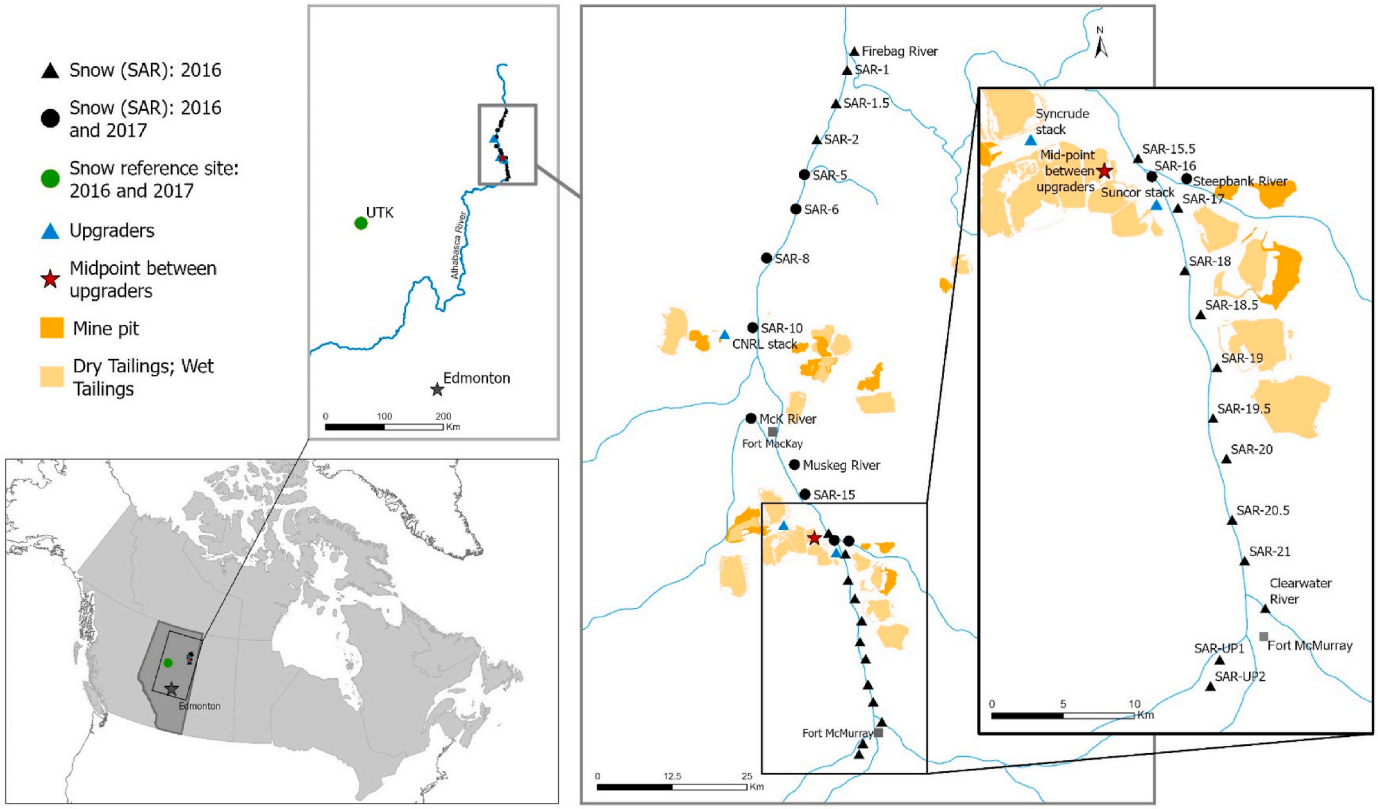

Fig. 1. Sampling locations in winter 2016 and 2017 along the Athabasca River (SAR), its tributaries, and at the reference site (UTK).

2.2. Trace element analysis

Concentrations of 16 TEs (Al, As, Be, Cd, Cs, La, Li, Mo, Ni, Pb, Sb, Sr, Th, Tl, V and Y) were determined using ICP-MS (iCAP RQ, Thermo Scientific). The limits of detection (LOD), quantification (LOQ), precision, and accuracy of the certified reference materials are listed in Table S2.

The values presented here are the average concentrations of TEs for the snow samples collected in triplicate. Comparison of the variation in TE concentrations in regard to depth of the snow samples was not undertaken, mainly because this is outside of the scope of the study. Also, in some cases the snow profile was not deep enough for evaluating this type of variability. For comparison between years and sites, some samples collected in 2017 were omitted or combined (Table S3). For example, site SAR-10.5 was excluded from the 2017 set due to the extremely low TE concentrations associated with the abundance of locally-derived sand probably from the large sandbar along this shore of the river (Barraza et al., 2024). In regard to sites SAR-16 and SAR-17, average concentrations were calculated based on sites SAR-16-E and SAR-16-W, and SAR-17 and SAR-17.5, respectively collected in 2017 (Barraza et al., 2024).

Trace elements are presented and discussed in 3 groups as follows: i) conservative (Al, Y, Th, La) and mobile lithophile elements (Li, Be, Cs, Sr) (Goldschmidt, 1937); (ii) elements enriched in bitumen (V, Ni, Mo) (Bicalho et al., 2017; Goldschmidt, 1937), and (iii) potentially toxic, chalcophile elements (As, Cd, Sb, Pb, Tl) (Goldschmidt, 1937; Javed et al., 2022).

2.3. Scanning electron microscopy and energy dispersive X-ray spectroscopy (SEM-EDS) analyses of the acid-insoluble fraction (>0.45 μm)

From selected snow samples, insoluble dust particles retained on PTFE membrane filters were examined for their size, morphology and major element chemical composition using a Field Emission Scanning Electron Microscope (Zeiss Sigma 300 VP-FESEM) equipped with an EDS system. Details of sample preparation and instrument settings can be found elsewhere (Barraza et al., 2024). Mineral identification was done using the chemical information obtained from the X-ray analysis, and relative abundances of each probable mineral phase were calculated based on the number of grains analyzed per site. The samples selected for SEM analyses correspond to the following sites and snow layers: SAR-5 (bottom), McKay River (top), SAR-16 (top, middle, bottom), Steepbank River (top, middle, bottom), SAR-17 (top, middle, bottom), SAR-20 (bottom), Clearwater River (top), SAR-UP2 (top), and UTK (top and bottom) (Fig. 1, Table S3).

2.4. Statistical analysis

All the statistical analyses were done using the R programming environment version 3.5. (R Core Team, 2021).

For the 2016 data, linear regressions were conducted to explore the specific correlations between certain elements (Barraza et al., 2024) using the *lm* function. For the 2016 and 2017 data, Pearson correlations were calculated after transformation for normality.

Principal component analysis (PCA) was used for a multivariate visual summary of TE concentrations in 2016 and 2017, implemented with the *princomp()* function. Each of the 16 TEs was individually log-transformed and, where applicable, a constant was added or subtracted prior to transformation to achieve normality prior to PCA analysis.

Further, a post-hoc effect size statistical test was carried out with four geographic groups, comparing the reference site (UTK) with sites near the two central upgraders (midstream; sample locations SAR-15 to SAR-18, including Steepbank River), as well as samples downstream (SAR-1 to SAR-10, including Firebag, McKay and Muskeg rivers) and upstream

from the upgraders (SAR-18.5 to SAR-UP2, including Clearwater River). A mixed effects model with year (2016 or 2017) being specified as a random factor and the sample groups (reference, midstream, upstream, and downstream) as fixed effect, was used. The dependent variables (16 TEs) were log-transformed prior to analysis, and 1-sided contrasts of the TE concentrations near the upgraders against the reference, upstream and downstream locations was carried out. An adjustment for multiple inferences was applied using the Dunn–Šidák correction (Šidák, 1967). Estimated means and effect size statistics were back-transformed to be reported in original units, and therefore represent estimates of median TE concentrations. The analysis was implemented using the *lmer* function for mixed models of the package *lme4* (Bates et al., 2015) in combination with the contrast function of the *emmeans* package (Lenth, 2016). Although the *lme4* package includes model options for non-parametric residuals, the *emmeans* package for effect size statistics does not. Since transformations to normality were unproblematic, this analytical option was chosen.

3. Results and discussion

3.1. Spatial variations in the concentrations of TEs in snow from the ABS region in 2016 and in 2017

The TE concentrations in snow tend generally to increase from downstream of industry (i.e. the Firebag River, at the north end of the transect) to the centre of industrial activity (i.e. at Steepbank River). Similarly, they increase from upstream of industry (i.e. SAR-UP2, at the south end of the transect) to the Steepbank River in 2016 and to SAR-17 in 2017 (Figs. 2 and 3; Figs. S2–S4; Table S3). The only exception is Sb in 2016, which increases from the Firebag River to SAR-17 and from SAR-UP2 to SAR-17 (Fig. S2c). These trends are in agreement with previous studies conducted in the same area (Gopalapillai et al., 2019; Guéguen et al., 2016; Kelly et al., 2010).

3.2. Interannual variations in the concentrations of TEs in snow from the ABS region

Overall, average concentrations of TEs in 2016 were in the range of 1.2 ng/L (Tl, which is the least abundant) to 1.7 mg/L (Al, the most abundant) (Table S3) and similar to the values reported in 2017 (Barraza et al., 2024). However, there are some exceptions such as TEs on sites SAR-5 and SAR-8, situated 61 and 47 km downstream of industry respectively (Fig. 1, Table S1). At the former site, TEs were 1.2–4.3x greater in 2016 than in 2017, whereas in the latter they were 1.2–5.7x greater in 2017 than in 2016 (Table S3).

These results could be related to differences in the precipitation and accumulation of snow as well as to thawing-freezing cycles (Colbeck, 1981) before the sampling took place. As mentioned in section 2.1, although there is no available data about snow on the ground in 2016, the temperature records in 2016 at the Mildred Lake station indicate more warmer days compared to 2017 (Government of Canada, 2022). This could have led to some melting and TEs becoming more concentrated (see Table S3) in some sections of the snow cover. The amount of dust deposited may also have varied, despite similar wind directions, because of slightly higher wind speeds in 2016 (Fig. S1). Variations in snow density (which was not measured), may also have played a role. All of these factors may help to explain some of the interannual variations in TE concentrations.

3.2.1. Conservative and mobile lithophile elements

In 2016, increases in Al and Y were in the range of 16–73 times from upstream or downstream to midstream of industry, whereas in 2017 the ranges were between 28 and 53 times (Fig. 2). A similar general trend is observed for Be, La, and Li in both years (Figures S2a, S3 and S4). By contrast, Sr and Th showed a more pronounced increase: up to 135-fold in 2016 and for Sr in 2017, up to 83-fold (Figs. S2a and S4).

3.2.2. Elements enriched in bitumen

In both years, the concentrations of V and Ni were similar, with increases in the range of 13–48 times (Fig. 2b–Table S3). Molybdenum is much less abundant in snow compared to V and Ni (Fig. S2b, Table S3), consistent with its much lower abundance in the ABS ores (Bicalho et al., 2017). However, in 2016, the increase in Mo was more pronounced than the other two elements (Fig. S2b, Table S3).

3.2.3. Potentially toxic chalcophile elements

Elements such as As, Cd, and Sb increased in the range of 3–6 times in 2016 and in the range of 12–20 times in 2017 (Fig. 3 and S2c, Table S3).

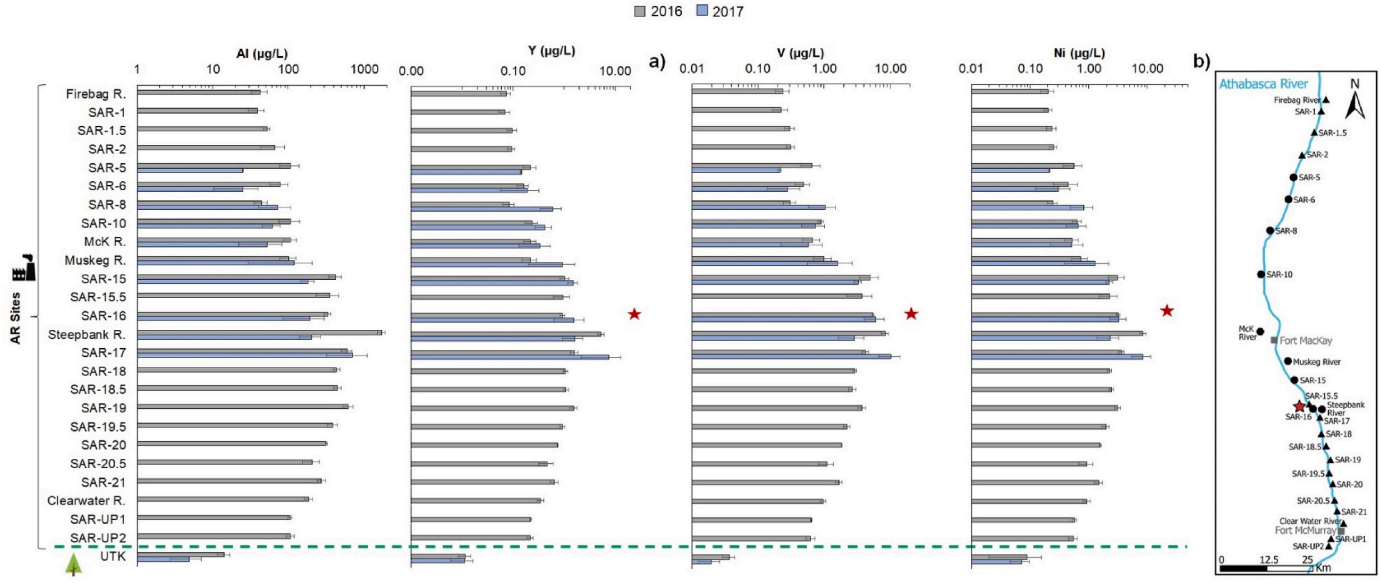

Fig. 2. Concentrations of **a)** conservative lithophile TEs (Al and Y) and **b)** elements enriched in bitumen (V and Ni) in the acid-soluble fraction of snow collected in the Athabasca River (SAR), its tributaries, and at the reference site (UTK) in winter 2016 (grey bars) and 2017 (blue bars). The red star represents the mid-point between the Syncrude and Suncor bitumen upgraders.
Note: The green dashed line separates the AR sites from the reference site.

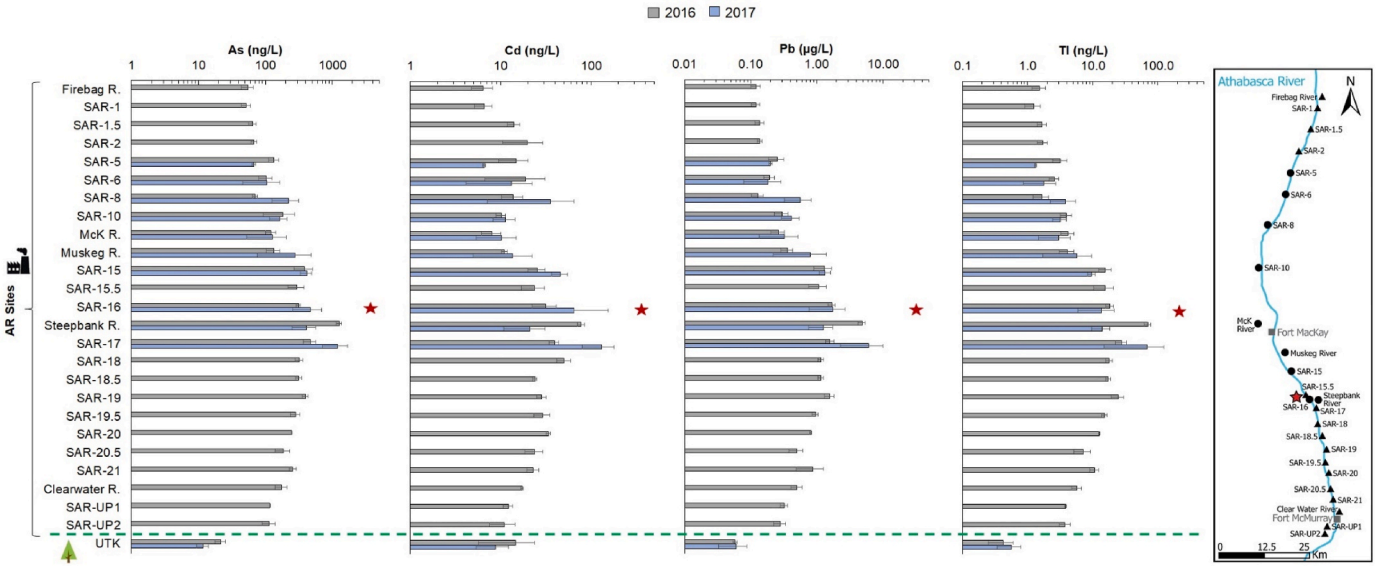

Fig. 3. Concentrations of chalcophile trace elements in the acid-soluble fraction of snow collected in the Athabasca River (SAR), its tributaries, and at the reference site (UTK) in winter 2016 (grey bars) and 2017 (blue bars). The red star represents the mid-point between the Syncrude and Suncor bitumen upgraders.
Note: The green dashed line separates the AR sites from the reference site.

Lead and Tl showed increases within the range of 5–14 in 2016 and 31 to 51 in 2017 (Fig. 3, Table S3).

3.3. Comparison between TE concentrations in snow from the ABS region and UTK, the reference site

3.3.1. Trace element ratios in snow from the ABS region relative to UTK in 2016

The average concentration of each TE in snow from the ABS region was normalized to its respective concentration in the snow from UTK (Table S4). The elements with the greatest ratios were Th (799) and Y (458) followed by V (228) and Mo (192) (Table S5). Contrarily, some of the chalcophile elements such as Cd and Sb had the lowest ratios ranging from 2 to 13 (Table S5), with the former dropping below 2 from midstream (SAR-15.5) to downstream (Firebag River) locations.

The sites with the lowest ratios relative to UTK are those located downstream of industry (sites: Firebag to Muskeg River) which is similar to what was observed in 2017 (Table S6).

3.3.2. Concentrations from upstream, midstream, and downstream of industry relative to UTK for two consecutive sampling years

A statistical analysis of TE levels in 2016 and 2017 was carried out for 3 post-hoc sample groups (midstream, upstream, and downstream of industry) relative to UTK. The analysis revealed that almost all TEs have significantly elevated levels (estimated median concentrations) relative to the reference site (Table 1). For example, considering the size of the standard error, Al is at least 138, 62.6 and 16.8 µg/L higher midstream, downstream, and upstream of industry respectively than at UTK.

At the locations near the two central upgraders, TEs were typically increased by one to two orders of magnitude, except for Cd and Sb (with only moderately but statistically significantly elevated levels) and Be (increase of three orders of magnitude) (Table 1). Locations upstream and downstream from this centre of industrial activity showed lower TE concentrations (2–10x), whereas the observed elevated levels of Cd at upstream and downstream locations were not statistically significant at an α-level of 0.05 (Table 1).

Table 1
Estimated median TE concentrations (in µg/L or *ng/L), and effect size statistics showing the minimum estimated increase relative to the reference site (UTK) at an α-level of 0.05 with Dunn-Šidák correction for multiple inference.

Element	Estimated median concentration				Minimum increase at 95% confidence		
	Reference	Midstream	Upstream	Downstream	Midstream	Upstream	Downstream
Al	8.34	386	196	64.1	≥138	≥62.6	≥16.8
As*	16.0	504	220	116	≥212	≥75.9	≥37.9
Be*	0.08	91.0	32.5	10.9	≥22.2	≥6.66	≥2.72
Cd*	11.3	42.7	21.1	13.1	≥7.48	n.s.	n.s.
Cs*	4.32	84.7	42.4	21.2	≥34.0	≥13.4	≥5.56
La	0.01	2.35	0.86	0.28	≥0.76	≥0.25	≥0.08
Li	0.01	0.91	0.49	0.17	≥0.30	≥0.13	≥0.04
Mo	<0.01	0.60	0.17	0.06	≥0.20	≥0.04	≥0.01
Ni	0.07	3.58	1.28	0.45	≥1.28	≥0.35	≥0.10
Pb	0.06	1.93	0.73	0.26	≥0.68	≥0.20	≥0.04
Sb*	5.48	48.8	44.5	15.8	≥16.7	≥12.9	≥1.92
Sr	0.48	22.0	11.3	2.50	≥5.42	≥2.36	≥0.21
Th	<0.01	0.48	0.18	0.04	≥0.13	≥0.04	≥0.01
Tl*	0.47	21.6	9.29	2.81	≥7.28	≥2.46	≥0.56
V	0.02	5.04	1.46	0.54	≥1.84	≥0.45	≥0.18
Y	0.01	1.86	0.72	0.22	≥0.59	≥0.20	≥0.06

Note: n.s. indicates a non-significant increase relative to the reference site.

3.4. Approaches to identify sources and TE behaviours in the ABS region

3.4.1. Linear regressions

The increase in the concentrations of V, Ni, As, Cd, Pb, and Tl in 2016 toward industry were proportional to the linear increase of Y (Table 2), an element used in the past as an indicator of mineral dust deposition (Shotyk, 2020; Stachiw et al., 2019). Only 2 elements, Mo (which is enriched in bitumen) and Sb (a chalcophile element) did not show this trend (Table 2). These results are largely in agreement with our previous findings (Barraza et al., 2024) suggesting that the main source of TEs in snow within the ABS area is from the mineral dusts generated both by industrial activities (i.e fugitive dusts) and natural sources such as river banks (Gopalapillai et al., 2019; Mamun et al., 2021; Shotyk et al., 2014).

3.4.2. Principal component analysis (PCA)

Generally, TE concentrations in snow were highly autocorrelated, with a single principal component explaining 91.2% of the total variance in log-transformed TE concentrations in the dataset (Fig. 4). As such, the value of a sample along the PC1 component can be interpreted as an index of overall contamination in terms of fugitive dusts emissions, with the sample locations on the right in Fig. 4 showing the highest level of TE concentrations. Given the predominance of conservative (Al, La, Th, Y) and other lithophile elements (Be, Li, Cs), PC1 is assumed to represent mineral dusts. Note that this PC1 is not linear because of variable transformations, and TE levels increase logarithmically from left to right. The analysis shows that the locations near the two central upgraders (SAR-15 to 18 and the Steepbank River locations) generally show the highest levels of TE concentrations, but also the nearby upstream locations (SAR 18.5, 19, 19.5) fall into this group. The group of TE vectors pointing toward the lower right highly correlate with Y, which can be interpreted as an indicator for dust-carried contamination.

Table 2
Correlations and linear regression equations between Y (conservative lithophile element) and TEs in the acid-soluble fraction of snow from the AR and its tributaries.

Type of TE	Correlations with Y (winter 2016 and 2017)	Linear regressions with Y (only winter 2016)
Conservative lithophile element	Al, r = 0.90	Al = 319(Y) + 52, R^2 = 0.99, p < 0.05
	La, r = 0.99	La = 1.19(Y) + 0.07, R^2 = 0.99, p < 0.05
	Th, r = 0.94	Th = 0.34(Y) + 0.0002, R^2 = 0.98, p < 0.05
Mobile lithophile elements	Be, r = 0.98	Be = 0.04(Y) + 0.01, R^2 = 0.94, p < 0.05
	Cs, r = 0.97	Cs = 0.04(Y) + 0.02, R^2 = 0.96, p < 0.05
	Li, r = 0.94	Li = 0.63(Y) + 0.11, R^2 = 0.98, p < 0.05
	Sr, r = 0.91	Sr = 13.6(Y) - 0.05, R^2 = 0.97, p < 0.05
Elements enriched in bitumen	Mo, r = 0.94	Mo = 0.21(Y) + 0.08, R^2 = 0.28, p = 0.05
	Ni, r = 0.90	Ni = 1.64(Y) + 0.40, R^2 = 0.67, p < 0.05
	V, r = 0.98	V = 1.71(Y) + 0.75, R^2 = 0.76, p < 0.05
Potentially toxic chalcophile elements	As, r = 0.98	As = 0.23(Y) + 0.07, R^2 = 0.98, p < 0.05
	Cd, r = 0.76	Cd = 0.01(Y) + 0.01, R^2 = 0.80, p < 0.05
	Pb, r = 0.97	Pb = 0.92(Y) + 0.15, R^2 = 0.97, p < 0.05
	Sb, r = 0.79	Sb = 0.007(Y) + 0.03, R^2 = 0.11, p < 0.05
	Tl, r = 0.96	Tl = 0.01(Y) + 0.002, R^2 = 0.98, p < 0.05

Note: number of sites in 2016 and 2017 = 35, number of sites in 2016 = 25.

Correlations of this group of vectors range from r = 0.90 to 0.99, including Mo (Table 2). This last element seems to have a mixed origin source: it is abundant in bitumen (Bicalho et al., 2017) but also used as a catalyst during bitumen upgrading (Galarraga and Pereira-Almao, 2010; Zhao et al., 2021). Depending on the sampling year and sampling locations, the PCA results for Mo may differ. For example, from our previous study, Mo did not show a significant correlation with Y probably because two sites with anomalous Mo concentrations were included in the statistical analysis (Barraza et al., 2024).

A second principal component PC2 indicates a subtle difference in TE behavior, accounting for an additional 2.7% of the variance. Only two TEs -Cd (r = 0.75) and Sb (r = 0.78)- have lower correlations with Y (Table 2) suggesting other emission sources. These two elements also show only moderately increased levels of concentrations at the samples near the upgraders (SAR 15–18), relative to the magnitude of increase in other TEs (Table 1). Previous studies in the area have reported that both elements are more abundant in the fine fraction of particulate matter (Landis et al., 2017; Mamun et al., 2022). The presence of Cd may be related to biomass burning (Mamun et al., 2021) which includes wood burning for residential heating and land clearing operations, both occurring in winter (Landis et al., 2017; Mamun et al., 2022). In the case of Sb, brake linings (Krachler et al., 2005b) and fossil fuel combustion (Tylenda et al., 2022) could be potential sources of this element in airborne particles. A recent study suggests that Sb in $PM_{2.5\text{-}10}$ is related to « non-oil sands » sources such as industrial processes and fuel combustion, residential wood burning, biogenic sources, and waste combustion (Yang et al., 2023). Most of the publications about Sb deposition also highlight its anthropogenic origin and transboundary transport (Krachler et al., 2005b; Pačes et al., 2023; Wiklund et al., 2020).

3.4.3. Trace element ratios

The ratios of selected TEs were used as follows to understand their geochemical behaviour in the acid-soluble snow fraction (Fig. 5 and S5): the ratios were compared to their respective ratios in the snow from UTK, the reference site, as well as the Upper Continental Crust (UCC) (Rudnick and Gao, 2014). Also, metal ratios in snow were compared to fly ash (Jang and Etsell, 2005), bitumen (Gosselin et al., 2010), petcoke (Gosselin et al., 2010; Shotyk, 2022), bulk ABS samples (Bicalho et al., 2017), the mineral fraction of the ABS (Bicalho et al., 2017), and soils of northeastern Alberta (Spiers et al., 1989). In addition, they were also compared to selected geological (such as soil and till) and industrial materials (such as dry tailings) sourced from the ABS region (Table S7). Although total concentrations of TEs in bulk snow are more commonly used for these calculations (Javed et al., 2017, 2022), the focus here is the acid soluble component.

First, the V/Ni ratios in snow were calculated to help identify the dominant source of these elements, given that they are both enriched in bitumen but lost from the organic fraction during upgrading. The average V/Ni in the snow of the AR is approximately 1.2. This ratio in snow is 2–3 times lower than the other ratios evaluated, and 3 to 5 times greater than their equivalent ratio at UTK (Fig. 5). Although the V/Ni ratio is similar to that of fly ash, there are several reasons why this is not the most likely source. First, fly ash is only generated at high temperatures i.e. during combustion of fossil fuels, and not at the temperatures of bitumen upgrading (see Jang and Etsell, 2005). Second, the installation of electrostatic precipitators on the bitumen upgraders in 1979, to reduce the emissions of particulate matter, caused an immediate decline in V atmospheric emissions, resulting in a ten-fold reduction of V concentrations in snowpack of the area at the time (Murray, 1981). Third, the enrichments of V and Ni in age-dated peat cores from bogs have been in decline for decades (Shotyk et al., 2017a). Fourth, SEM analyses of the ash fraction of those peat cores only detected fly ash particles in peat pre-dating the installation of the precipitators.

Finally, the petroleum industry has been phasing out the use of coke as fuel for the upgraders, and transitioning to natural gas. In summary, the V/Ni ratios in snow indicate that V is underrepresented in the snow

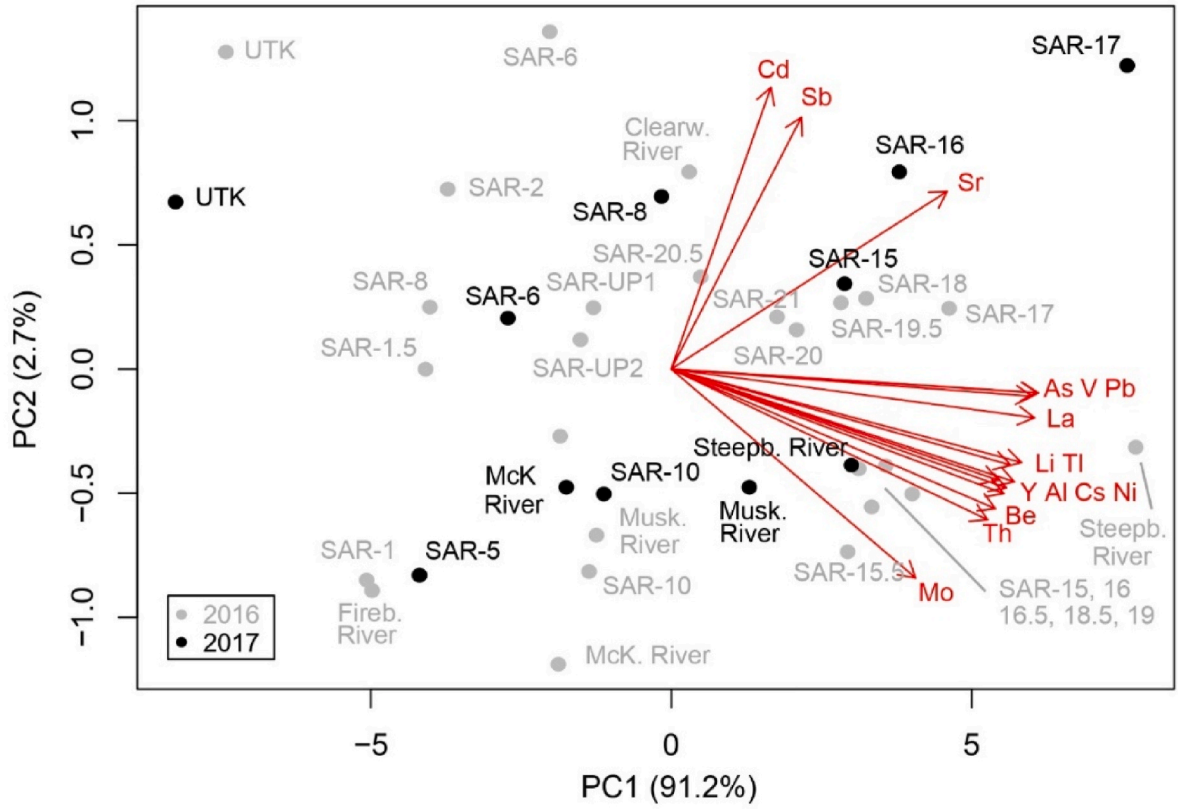

Fig. 4. Principal component analysis (PCA) of TE concentrations in the acid-soluble fraction of snow assessed in the years 2016 and 2017.
Note: abbreviations refer to sample locations as shown in Fig. 1.

in comparison to Ni, relative to the composition of bitumen, bulk ABS ores, and coke. Similar findings were reported earlier in snow collected from ombrotrophic bogs in the ABS region (Javed et al., 2022). Vanadium and Ni in bitumen are both predominantly in the form of porphyrins, however the V compounds are more volatile than those of Ni (Hodgson, 1954). Thus, an enrichment of V in atmospheric aerosols during bitumen upgrading, relative to Ni, could reasonably be expected.

The results of the snow analyses, however, suggest that the reverse is true, and that Ni is emitted preferentially over V. When compared to the geomaterials, only the road construction material (type 1) has a similar V/Ni to that of snow. In fact, road dusts of the area contain much greater concentrations of V and Ni than do tailing sands (Edgerton et al., 2012; Landis et al., 2012). Although it is a common practice in Alberta to use hydrocarbon-based dust suppressant to control airborne particulate matter from unpaved roads (Government of Alberta, 2012), the V/Ni ratios of the snow are a good match for road construction materials which have been shown to be an important source of fugitive dusts in the ABS region (Landis et al., 2012; Wang et al., 2015; Xing and Du, 2017). While the V/Ni ratios in snow indicate a mixture of dust sources in the area, quantifying the relative contribution from each is more difficult.

The V/Y and Ni/Y ratios were also calculated in order to determine the enrichment of V and Ni relative to Y, an element assumed to be derived mainly from mineral material (Fig. 5). Only two sites (SAR-16 and SAR-15, in 2016; calculated from Table S3) have V/Y ratios above the UCC, and two sites were similar to the ratios observed in tailings (Muskeg River and SAR-15, in 2016; calculated from Table S3): the rest are similar to the ratios observed at UTK. By contrast, the Ni/Y ratios at the AR sites were above the UCC in 2016 and similar to the bulk ABS (midstream locations). While these findings point to dusts generated directly by open-pit bitumen mining, Ni/Y in the AR snow samples are lower than those in the snow from UTK (Fig. 5). So, regardless of the sources of V and Ni to the snow of the AR, the metal/Y ratios here, compared to UTK, show that enrichments of V and Ni, if they exist at all, are small.

Conservative, lithophile elements which are enriched in heavy minerals of the ABS (Fustic et al., 2021; Mellon, 1956; Roth et al., 2017), as well as froth treatment tailings, were also examined (Ciu et al., 2003; Gosselin et al., 2010; Roth et al., 2017). Specifically, La, Th, and Y which are enriched in heavy minerals were normalized to Al concentrations: Al is enriched in much lighter aluminosilicates, and is commonly used in weathering studies as an indicator of the abundance of clays. In fact, Al increases in concentration with the clay content of the ABS (Donkor et al., 1996; Shotyk et al., 2014). Thus, ratios of La, Y and Th to Al are indices of the relative abundance of heavy minerals compared to light minerals. Lanthanum was also normalized to Y to evaluate our data and our approach, given that both elements are enriched in heavy minerals. When comparing these ratios in snow of the AR to the snow of UTK and the UCC, only the La/Y ratios have similar values, as would be expected. The other ratios (i.e. La/Al, Y/Al, and Th/Al) are 2–5 times greater in the AR snow compared to UTK and 6 to 30 times greater than the crustal ratios (Fig. 5 and S5). Further, these indices (of the ratios of heavy minerals to light minerals) are 4–33 times greater in the snow than the tailings (Fig. 5 and S5, Table S7). Given that these ratios in snow exceed their crustal ratios, heavy minerals must be preferentially enriched in the snow of the AR, compared to light minerals. The considerable chemical stability of the heavy minerals (e.g. monazite, rutile, zircon) helps to explain the limited chemical reactivity of the dusts of the ABS region.

3.5. *Mineralogical composition of the insoluble dust particles and its influence on the chemical reactivity of TEs*

3.5.1. *Size, morphology, and particle classification*

The SEM analyses performed on selected PTFE filters containing the

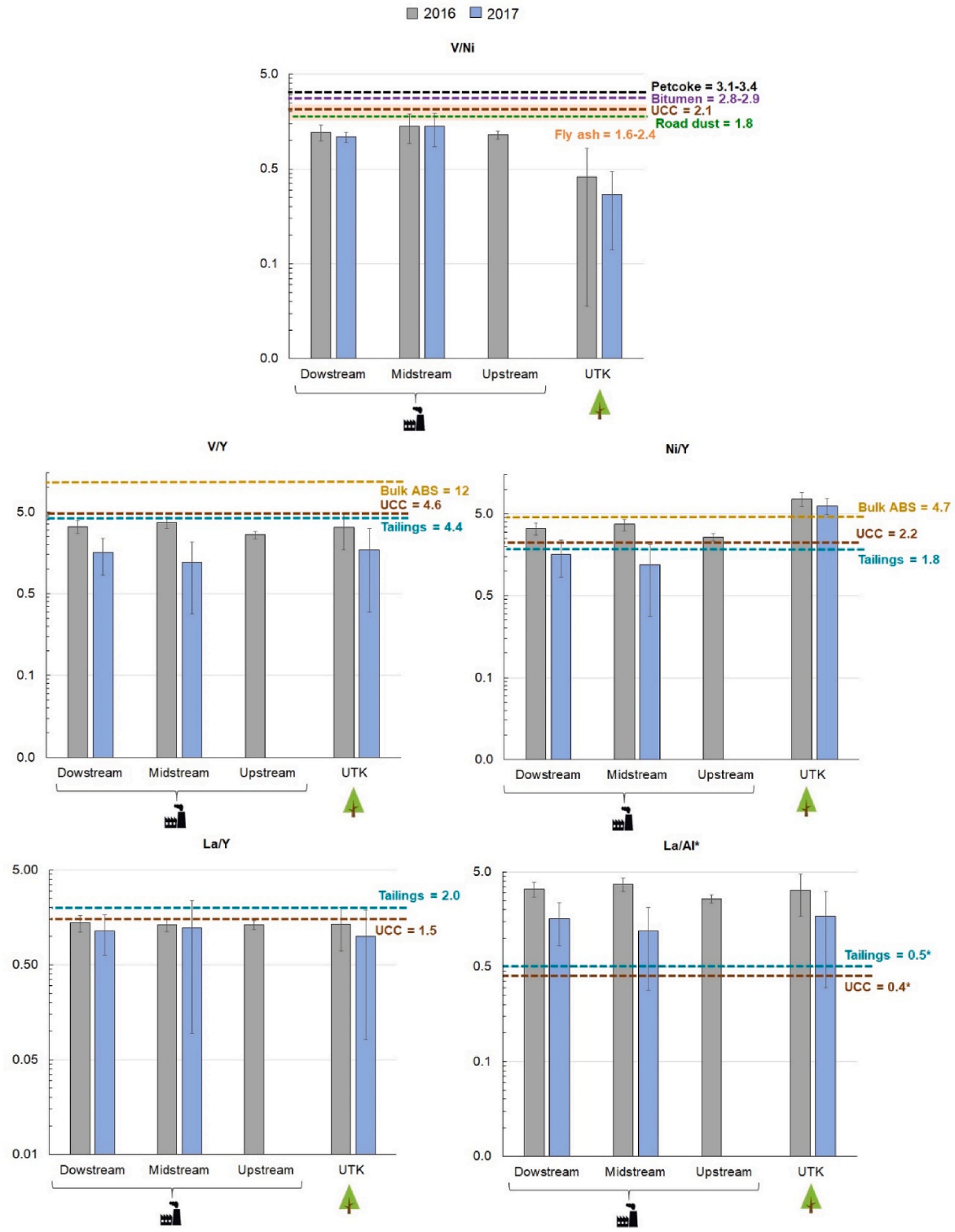

Fig. 5. Average V/Ni, V/Y, Ni/Y, La/Y, and La/Al* ratios (±SE) in the acid-soluble fraction of snow collected in the Athabasca River (downstream, midstream, and upstream of industry), and at the reference site (UTK) in winter 2016 (grey bars) and 2017 (blue bars).

Notes: The dashed lines represent: brown = TE ratios in the Upper Continental Crust (UCC) according to Rudnick and Gao (2014), purple = V/Ni in bitumen according to Gosselin et al. (2010) and Bicalho et al. (2017), black = V/Ni in petcoke according to Gosselin et al. (2010) and from unpublished data (analyzed in the SWAMP laboratory, June 2015; Shotyk, 2022), green = V/Ni in road dust (type 1, from unpublished data, see Table S7 for more information), turquoise = ratios in tailings (see Table S7), dark yellow = ratios in bulk ABS from Bicalho et al. (2017). The light orange area represents the V/Ni in fly ash according to Jang and Etsell (2005). (*) To obtain the actual La/Al ratios, the values have to be multiplied by a factor of 10^{-3}. Not included in the figure for visibility reasons are the values of V/Ni in: bulk ABS samples (2.6) (Bicalho et al., 2017), mineral fraction of the bitumen (2.3)(Bicalho et al., 2017), and soils in northeast Alberta (3.2) (Spiers et al., 1989).

insoluble particulate fraction (>0.45 μm) showed that particles were irregularly-shaped, in the range of 20–200 μm, and that there were numerous microaggregates (Appendix A, selected images). Consistent with our previous observations (Barraza et al., 2024), larger particles were more abundant at the midstream sites compared to locations farther south (upstream of industry) or north (downstream). The mineral identification, based on the elemental composition obtained from the EDS spectra, is summarized in Table S8 and Fig. S6. One of the challenges associated with the accurate characterization of minerals using SEM, even in combination with XRD analysis, is that dust particles are usually found in the form of aggregates rather than in pure mineral forms (Panta et al., 2023). In addition, the limited number of particles examined and the small amounts of sample on each filter make the calculation of mineral abundances difficult. Therefore, the mineral phases presented here may not be the only ones, and their estimated abundances should be considered qualitative. Overall, the insoluble dust particles consist of quartz, clays, micas, feldspars, oxides, and sulphur-rich minerals as previously reported (Barraza et al., 2024), in agreement with the composition of the mineral fraction of the ABS (Bayliss and Levinson, 1976; Bichard, 1987; Kaminsky et al., 2006; Mossop, 1980; Osacky et al., 2013). Compared to the 2017 snow samples (Barraza et al., 2024), those collected in 2016 (this study) contain fewer S-rich particles, some phosphate minerals, and some Sn, Cu, and Zn-rich particles. Research about sulphur emissions and deposition in the ABS region is usually related to gaseous emissions (SO_2) (Bari et al., 2020; Edgerton et al., 2020) and to a lesser extent, particulate S (sulphate$^-$ and elemental S) (Edgerton et al., 2020; Yang et al., 2023). Although ambient S is higher near the center of oil sand operations, gaseous S concentrations have been declining since 2000 (Edgerton et al., 2020) which may be also the case for S in PM_{10} and $PM_{2.5}$. Information about the amount of S stockpiled in the area is scarce making it difficult to estimate the possible importance of wind-blown, particulate sulphur. By contrast, 10^8 tons of petroleum coke – which typically is 6–8% by weight S (Phillips and Chao, 1977)- are stockpiled in the ABS region resulting in the spread of fine particles through aeolian transport (Nesbitt and Lindsay, 2017; Zhang et al., 2016). Another potential source of S could be trace amounts of pyrite (Bayliss and Levinson, 1976; Osacky et al., 2013) which is also found in the mineral fraction of the ABS.

Phosphate minerals such as monazite - which contains rare earth elements – and apatite have been identified in oil sands tailings (Ciu et al., 2003; Kaminsky et al., 2008; Nesbitt et al., 2017) and in the mineral fraction of the bitumen respectively (Conybeare, 1966). Tin is rarely mentioned in existing literature of the area, but it has been reported in $PM_{2.5\text{-}10}$ (Yang et al., 2023). This element occurs mainly as cassiterite, SnO_2, a dense, refractory mineral (Angadi et al., 2015; Masau et al., 2000) which becomes enriched in highly weathered residua, such as the « sand » fraction of the ABS.

In summary, the results presented here (2016 snow samples) and earlier (2017 snow samples, Barraza et al., 2024) indicate that dust emissions are dominated to a great extent by insoluble silicates (Fig. S6, Table S8), with minor amounts of carbonates, phosphates, and sulphides. Detailed investigations of the pH-dependent release of TEs from these minerals, and the influence of particle size, are warranted.

3.5.2. *Acid solubility of TEs*

The acid solubility is expressed as the percentage of the total concentrations of TEs which are acid-soluble. The 16 TEs analyzed were included (Fig. 6), irrespective of the recoveries obtained from sediment and soil reference materials (Barraza et al., 2024; Javed et al., 2020).

Some of the most soluble elements such as Pb, Cd, Sr, Y, La and Sb occur in carbonate minerals (Smrzka et al., 2019). In the case of As, it can be incorporated into carbonates, as well as sulfides, and Fe-oxy (hydroxide) minerals (Möller and De Lucia, 2020; Smrzka et al., 2019; Wang and Putnis, 2020; Zhang et al., 2020). Over half of the occurring Be-minerals are silicates (Bolan et al., 2023; Vesely et al., 2002), although it also may occur in carbonate minerals (Pekov et al., 2008). Carbonate minerals such as calcite and dolomite were identified in selected unacidified bulk snow samples using X-ray diffraction (unpublished data) from sites SAR-15, SAR-15.5, SAR-16, Steepbank River, SAR-18, SAR-19 and Clearwater River. These minerals, in addition to siderite, are abundant in the mineral fraction of the ABS (Bichard, 1987; Osacky et al., 2013). Besides, elevated concentrations of Ca and Mg were

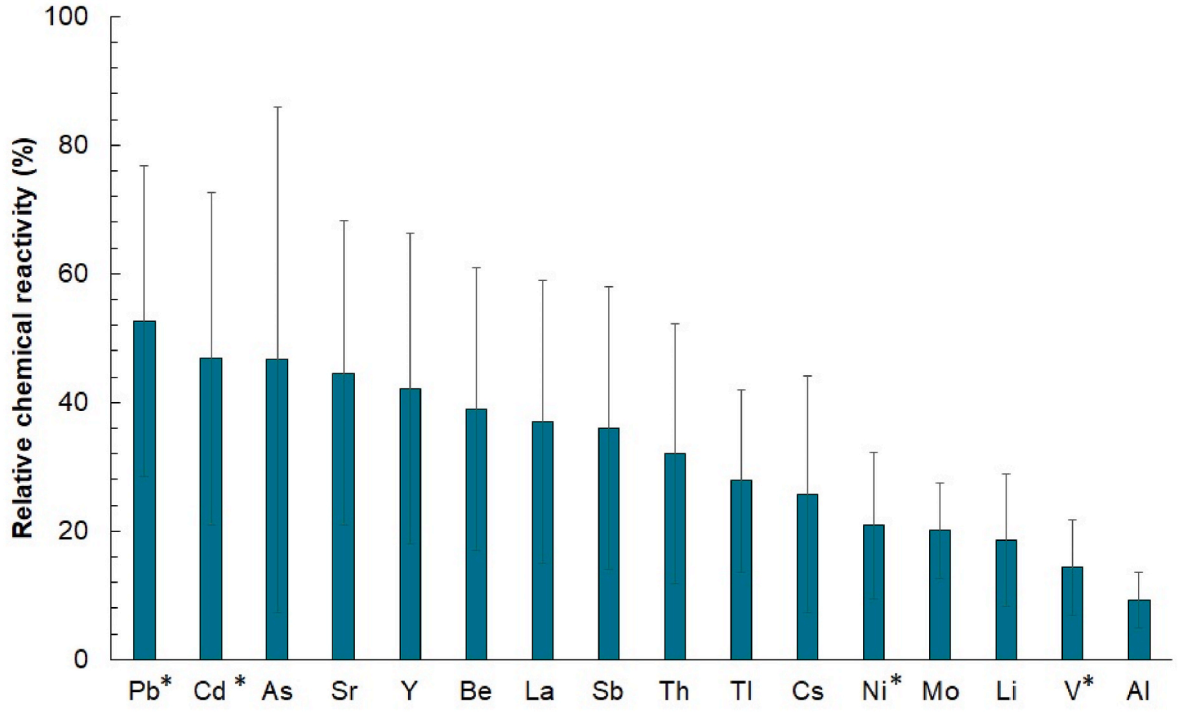

Fig. 6. Relative acid solubility (%) of TEs in 2016, calculated from the ratio of acid-soluble to total concentrations.
Notes: The error bars represent the standard deviation. The asterisks are assigned to elements with acceptable recoveries (Barraza et al., 2024).

found in the particulate fraction of snow at SAR-1 and from SAR-15 to SAR-20.5 (unpublished data). Nevertheless, the sites with the highest reactivities for this group of elements are those located between Steepbank River and SAR-UP2, upstream of industry (Table S9).

The elements of intermediate solubility -Th, Tl, and Cs- (Fig. 6) probably occur in silicates and are partly soluble, only because of the strength of acid used to leach them.

At the opposite extreme of acid solubility are Al, V, Li, Mo and Ni (Fig. 6). Aluminum and Li are mainly associated with clay minerals and silicates (Simon and Anderson, 1990; Starkey, 1982; Tadesse et al., 2019), both of which have limited solubility. Vanadium, Ni and Mo occur in petcoke in the ABS region to the extent of 1680, 500 and 66 mg/kg respectively (Gosselin et al., 2010; Shotyk, 2022). They may also be deposited in the form of fly ash which, we assume, has limited solubility in acid. Vanadium in petcoke is dominated by V (IV) porphyrin complexes which are usually resistant to weathering and thermal decomposition (Nesbitt and Lindsay, 2017; Zuliani et al., 2016). Similarly, Ni speciation is dominated by porphyrin complexes (Nesbitt et al., 2017). However, V and Ni associated with the minor inorganic fraction are expected to be less stable and potentially more susceptible to weathering (Nesbitt et al., 2017). On average, 21 and 14% of V and Ni respectively were soluble, almost three times as much as reported in 2017 (Barraza et al., 2024). Regarding Mo, it has been observed that despite having lower concentrations than V and Ni in fluid coke, its leachability in water and solutions with high salt contents is relatively higher (Robertson et al., 2019). Moreover, Mo is used as a catalyst during bitumen upgrading, mainly under the form of MoS_2 which by contrast, has limited solubility (Robertson et al., 2019). Therefore, the behaviour of Mo may be due to a combination of dust particles emitted from both sources.

3.6. Ecological significance of TE emissions from bitumen mining and upgrading

3.6.1. Significance of mineralogy and acid solubility of dusts for TEs in the Athabasca River (AR)

The TEs with greatest acid solubility (Pb to Sb, Fig. 6) appear to be associated with carbonate minerals. While these minerals dissolve in strong acid (pH $<$ 1), the pH of the AR lies within the range 6.8–8.5 (Fiera, 2013; Ghotbizadeh et al., 2022), with the lower values due to spring snowmelt. Given the pH of the water and the abundance of Ca and bicarbonate (20–50 mg/L and 100–200 mg/L in summer and winter, respectively; Fiera, 2013), and considering the solubility of calcium carbonate (Chou et al., 1989; Deocampo, 2010), it seems that the AR is saturated in respect of that mineral phase. Thus, any TEs associated with carbonate mineral dusts may have little relevance for this aquatic ecosystem, as the particles themselves are not expected to dissolve in the river water. Moreover, the pH of the AR water is well buffered against changes due to the abundance of dissolved bicarbonate; this species (HCO_3^-) is converted to carbonic acid (H_2CO_3) as hydrogen ions (H^+) are added to the river (e.g. during spring snowmelt), thereby constraining the change in pH of the water (Fiera, 2013). In regard to the presumed silicate mineral fraction of the dusts, again the ecological relevance of TEs contained therein should be minimal, given the generally low abundance of TEs in the minerals, and their limited reactivity in all but the most corrosive fluids.

3.6.2. The examples of Li and be

Beryllium is commonly reported as a toxic TE (Bolan et al., 2023; Pawlas and Pałczyński, 2022; Taylor et al., 2003), and is classified as probable human carcinogen. Concerns arise mainly regarding inhalation exposure (ATSDR, 2023; Stearney et al., 2023), but the mechanisms of toxicity are not well understood (Buchner, 2020; Elguero and Alkorta, 2023). In the case of Li, some studies present adverse impacts while others report beneficial effects in living organisms (Bernard, 2022; Shahzad et al., 2017). Within the context of the environmental impacts of bitumen mining and upgrading on these two metals, the most relevant questions are regarding the quantities released, their chemical form, and their bioaccessibility and bioavailability in aquatic environments.

The concentrations of Li and Be in the acid-soluble fraction of snow collected along the AR, are certainly much greater than those found at the reference site (UTK) (Figs. S3 and S4). However, it is a considerable challenge to establish the «background » concentrations of these elements, even for state-of-the-art ICP-MS operating in a metal-free, ultraclean lab, simply because the concentrations in snow from the reference site are typically below the LOD or LOQ (Table S4).

Evidently, both elements are more abundant in snow collected from the industrial zone, relative to sites downstream (i.e. from SAR-2 to the Firebag River) (Figs. S3 and S4). Thus, emissions of particulate matter from bitumen mining and upgrading are certainly contributing both of these elements to the environment. Comparing Li to Cs (both form monovalent cations in solution) and Be to Sr (which both form divalent cations) provide additional insights. These 4 elements increase approximately by a factor of 10 from upstream of industry, toward the industrial zone, as well as toward industry from downstream locations (Figs. S3 and S4). The Li/Cs and Be/Sr ratios in snow compared to the UCC (Rudnick and Gao, 2014) suggest that there is approximately twice as much Li in the snow, relative to Cs, but only 2/3 of the Be relative to Sr, as one would expect based on the deposition of dusts consisting of rock-derived mineral matter (Figs. S3 and S4). For additional perspective, at UTK, these ratios are 1.3 to 5x lower than the corresponding values for the UCC, and 11 to 5x lower than at the AR sites.

To obtain a sense of the extent to which Li and Be are enriched toward industry in natural waters of the area, there is now data available for these elements in peat bog porewaters which represent the most acidic (pH 4) natural waters of the region. Here, we find that Li and Be concentrations do increase with distance toward industry (Shotyk et al., 2023), but the concentrations in the bog waters are at or below the values typical of freshwaters, and lower than the concentrations found in the acid-soluble snow (Table S10).

In regard to other studies of snow, Kelly et al. (2010) reported particulate Be and total plus dissolved Be were presented by Guéguen et al. (2016) who also reported total and dissolved concentrations of Li. Loads of both elements from snowmelt to surface waters was published by Gopalapillai et al. (2019): they suggested that Be may be associated with raw oil sand dusts and Li with road dusts. It would be help to compare the concentrations of these elements in snow with the corresponding data for the dissolved fraction of the AR, but published data for Li and Be in surface waters of the area is scarce (Ghotbizadeh et al., 2022; Javed and Shotyk, 2018; Shotyk et al., 2017b). From our own data (published and unpublished), the concentrations in the river are approximately 9x lower (Be) and 9x greater (Li) than the concentrations in the acid soluble snow of 2016. In 2017 the concentrations in the river are 18x lower (Be) and 9x greater (Li) (Table S10). These results suggest that dust particles in snow cannot contribute significantly to the dissolved concentrations of Li in the surface waters of the AR during spring snowmelt, simply because it is already much more abundant in the river. Regarding Be, our snow data represents results obtained after leaching the samples in 0.5 % HNO_3. It would be helpful to know how much of the total Be in snow is contained in the filterable fraction (i.e. $<$ 0.45 μm), as this would provide a better guide to its potential bioaccessibility in the river during snowmelt.

4. Summary and conclusions

Trace elements in the acid-soluble fraction of snow collected on the AR and its tributaries located in the ABS region, showed considerable spatial variation, with increasing concentrations closer to the bitumen mining and upgrading operations. Even though the concentrations of most of the 16 TEs determined were similar over two consecutive sampling years (2016 and 2017), some elements exhibited higher values at specific locations in one of the two years. Compared to the reference

site UTK, located 264 km SW from the industrial area, sites located downstream, midstream, and upstream of industry showed greater TE concentrations, especially regarding the conservative elements (i.e. Al, Th, Y) which are indicators of local mineral dusts, as well as some of the elements enriched in bitumen (V and Mo).

Using linear regressions with Y, specific TE ratios, and PCA as an approach to elucidate potential sources of these elements, it is clear that dust particles of diverse origin (industrial activities and natural sources), chemical composition and reactivity, are present in the snow. However, elements such as Cd and Sb appear to be far less affected or unaffected by these dusts, and may have other sources not linked to the ABS industry.

Further investigation is needed to identify the minerals in local dusts. It is expected that the minerals hosting TEs are mainly those found in the inorganic fraction of the ABS. So far, the presence and relative abundance of insoluble silicate minerals such as quartz may explain the low TE concentrations observed, and also their limited acid solubility. For instance, only between 21 and 14% of V and Ni respectively could be liberated from these dust particles using 0.5% of HNO_3. Carbonate minerals dissolve during the extreme pH conditions employed here (pH < 1), and release any TEs they may contain. However, the potential to release some of these TEs into the surface waters of the AR and its tributaries is minimal given the fact that this river is saturated in respect to calcium carbonate. Finally, the assessment of the potential environmental impact of elements such as Be represents a challenge from the analytical point of view due to the extremely low concentrations in snow from the reference site. Despite the fact that a previous study suggested that Be is being released to the AR from bitumen mining and upgrading, extremely corrosive leaching conditions are needed to generate Be in concentrations that exceed (9–18 times) the dissolved concentrations in the river. More research is needed to quantify the range in concentrations of Be in the filterable fraction (i.e. < 0.45 μm) of the snow, as this would provide more information regarding its bioaccessibility in aquatic environments.

Funding sources

This study is part of the Metals vs Minerals project funded by the Natural Sciences and Engineering Research Council of Canada (NSERC) and the Canada's Oil Sands Innovation Alliance (COSIA).

CRediT authorship contribution statement

Fiorella Barraza: Data curation, Formal analysis, Investigation, Methodology, Supervision, Validation, Visualization, Writing – original draft. **Andreas Hamann:** Data curation, Visualization, Writing – review & editing. **Tommy Noernberg:** Methodology, Writing – review & editing. **Judy Schultz:** Formal analysis, Methodology, Writing – review & editing. **William Shotyk:** Conceptualization, Funding acquisition, Investigation, Methodology, Project administration, Supervision, Writing – review & editing.

Declaration of competing interest

The authors declare that they have no known competing financial interests or personal relationships that could have appeared to influence the work reported in this paper.

Acknowledgements

The authors wish to thank John Brogly from COSIA and Brett Purdy from Alberta Innovates. We are grateful to Dr. Mark Donner for outstanding support in the field, to Dr. Michael Powell for the discussions about mineralogy identification using SEM, for administrative support to Tracy Gartner and Karen Lund, for proofreading to Sandor Haas-Neill and Andy Luu, for creating the map to Rick Pelletier. We also want to acknowledge the technical staff at the SWAMP laboratory, especially Kailee Goertzen, for the time invested in cleaning supplies and processing samples.

Appendix A. Supplementary data

Supplementary data to this article can be found online at https://doi.org/10.1016/j.apr.2024.102244.

References

Adebiyi, A., Kok, J.F., Murray, B.J., Ryder, C.L., Stuut, J.-B.W., Kahn, R.A., Knippertz, P., Formenti, P., Mahowald, N.M., Pérez García-Pando, C., Klose, M., Ansmann, A., Samset, B.H., Ito, A., Balkanski, Y., Di Biagio, C., Romanias, M.N., Huang, Y., Meng, J., 2023. A review of coarse mineral dust in the Earth system. Aeolian Res. 60, 100849 https://doi.org/10.1016/j.aeolia.2022.100849.

Angadi, S.I., Sreenivas, T., Jeon, H.-S., Baek, S.-H., Mishra, B.K., 2015. A review of cassiterite beneficiation fundamentals and plant practices. Miner. Eng. 70, 178–200. https://doi.org/10.1016/j.mineng.2014.09.009.

ATSDR, 2023. Agency for toxic substances and disease registry. Toxic substances portal. Beryllium. Toxicological Profile 274. https://wwwn.cdc.gov/tsp/ToxProfiles/ToxProfiles.aspx?id=1441&tid=33, 1.4.24.

Barbante, C., Spolaor, A., Cairns, W.R., Boutron, C., 2017. Man's footprint on the Arctic environment as revealed by analysis of ice and snow. Earth Sci. Rev. 168, 218–231. https://doi.org/10.1016/j.earscirev.2017.02.010.

Bari, M.A., Kindzierski, W.B., Roy, P., 2020. Identification of ambient SO2 sources in industrial areas in the lower Athabasca oil sands region of Alberta, Canada. Atmos. Environ. 231, 117505 https://doi.org/10.1016/j.atmosenv.2020.117505.

Barnhart, B., Flinders, C., Ragsdale, R., Johnson, G., Wiegand, P., 2021. Deriving human health and aquatic life water quality criteria in the United States for bioaccumulative substances: a historical review and future perspective. Environ. Toxicol. Chem. 40, 2394–2405. https://doi.org/10.1002/etc.5130.

Barraza, F., Javed, M.B., Noernberg, T., Schultz, J., Shotyk, W., 2024. Spatial variation and chemical reactivity of dusts from open-pit bitumen mining using trace elements in snow. Chemosphere, 141081. https://doi.org/10.1016/j.chemosphere.2023.141081.

Bates, J.T., Weber, R.J., Abrams, J., Verma, V., Fang, T., Klein, M., Strickland, M.J., Sarnat, S.E., Chang, H.H., Mulholland, J.A., Tolbert, P.E., Russell, A.G., 2015. Reactive oxygen species generation linked to sources of atmospheric particulate matter and cardiorespiratory effects. Environ. Sci. Technol. 49, 13605–13612. https://doi.org/10.1021/acs.est.5b02967.

Bayliss, P., Levinson, A.A., 1976. Mineralogical review of the Alberta oil sand deposits (lower cretaceous, mannville group). Bull. Can. Petrol. Geol. 24, 211–224. https://doi.org/10.35767/gscpgbull.24.2.211.

Bergametti, G., Forêt, G., 2014. Dust deposition. In: Knippertz, P., Stuut, J.-B.W. (Eds.), Mineral Dust: A Key Player in the Earth System. Springer, Netherlands, Dordrecht, pp. 179–200. https://doi.org/10.1007/978-94-017-8978-3_8.

Bernard, A., 2022. Lithium. In: Handbook on the Toxicology of Metals. Elsevier, pp. 495–500. https://doi.org/10.1016/B978-0-12-822946-0.00018-0.

Bicalho, B., Grant-Weaver, I., Sinn, C., Donner, M.W., Woodland, S., Pearson, G., Larter, S., Duke, J., Shotyk, W., 2017. Determination of ultratrace (<0.1 mg/kg) elements in Athabasca Bituminous Sands mineral and bitumen fractions using inductively coupled plasma sector field mass spectrometry (ICP-SFMS). Fuel 206, 248–257. https://doi.org/10.1016/j.fuel.2017.05.095.

Bichard, J.A., 1987. Oil Sands Composition and Behaviour Research: the Research Papers of John A. Bichard, 1957-1965, AOSTRA Technical Publication Series. Alberta Oil Sands Technology and Research Authority, Edmonton, Alta., Canada.

Bogardi, J.J., Leentvaar, J., Sebesvári, Z., 2020. Biologia Futura: integrating freshwater ecosystem health in water resources management. Biol. Futura 71, 337–358. https://doi.org/10.1007/s42977-020-00031-7.

Bolan, S., Wijesekara, H., Tanveer, M., Boschi, V., Padhye, L.P., Wijesooriya, M., Wang, L., Jasemizad, T., Wang, C., Zhang, T., Rinklebe, J., Wang, H., Lam, S.S., Siddique, K.H.M., Kirkham, M.B., Bolan, N., 2023. Beryllium contamination and its risk management in terrestrial and aquatic environmental settings. Environ. Pollut. 320, 121077 https://doi.org/10.1016/j.envpol.2023.121077.

Boutron, C.F., 1990. A clean laboratory for ultralow concentration heavy metal analysis. Fresen. J. Anal. Chem. 337, 482–491. https://doi.org/10.1007/BF00322850.

Buchner, M.R., 2020. Beryllium-associated diseases from a chemist's point of view. Z. Naturforsch. B Chem. Sci. 75, 405–412. https://doi.org/10.1515/znb-2020-0006.

Carling, G.T., Fernandez, D.P., Johnson, W.P., 2012. Dust-mediated loading of trace and major elements to Wasatch Mountain snowpack. Sci. Total Environ. 432, 65–77. https://doi.org/10.1016/j.scitotenv.2012.05.077.

Carling, G.T., Tingey, D.G., Fernandez, D.P., Nelson, S.T., Aanderud, Z.T., Goodsell, T.H., Chapman, T.R., 2015. Evaluating natural and anthropogenic trace element inputs along an alpine to urban gradient in the Provo River, Utah, USA. Appl. Geochem. 63, 398–412. https://doi.org/10.1016/j.apgeochem.2015.10.005.

CCME, 2023. Canadian Council of ministers of the environment. Canadian environmental quality guidelines. Water-Aquat. Life. https://ccme.ca/en/resources/water-aquatic-life, 5.19.23.

Checketts, H.N., Carling, G.T., Fernandez, D.P., Nelson, S.T., Rey, K.A., Tingey, D.G., Hale, C.A., Packer, B.N., Cordner, C.P., Dastrup, D.B., Aanderud, Z.T., 2020. Trace element export from the critical zone triggered by snowmelt runoff in a montane watershed, Provo River, Utah, USA. Front. Water 2, 578677. https://doi.org/10.3389/frwa.2020.578677.

Cheng, I., Al Mamun, A., Zhang, L., 2021. A synthesis review on atmospheric wet deposition of particulate elements: scavenging ratios, solubility, and flux measurements. Environ. Rev. 29, 340–353. https://doi.org/10.1139/er-2020-0118.
Chou, L., Garrels, R.M., Wollast, R., 1989. Comparative study of the kinetics and mechanisms of dissolution of carbonate minerals. Chem. Geol. 78, 269–282. https://doi.org/10.1016/0009-2541(89)90063-6.
Ciu, Z., Liu, Q., Etsell, T.H., Oxenford, J., Coward, J., 2003. Heavy minerals in the Athabasca oil sands tailings-potential and recovery processes. Can. Metall. Q. 42, 383–392. https://doi.org/10.1179/cmq.2003.42.4.383.
Colbeck, S.C., 1981. A simulation of the enrichment of atmospheric pollutants in snow cover runoff. Water Resour. Res. 17, 1383–1388. https://doi.org/10.1029/WR017i005p01383.
Conybeare, C.E.B., 1966. Origin of Athabasca oil sands: a review. Bull. Can. Petrol. Geol. 14, 145–163. https://doi.org/10.35767/gscpgbull.14.1.145.
Davies, T.D., Abrahams, P.W., Tranter, M., Blackwood, I., Brimblecombe, P., Vincent, C. E., 1984. Black acidic snow in the remote Scottish Highlands. Nature 312, 58–61. https://doi.org/10.1038/312058a0.
Davis, R.E., 1991. Links between snowpack physics and snowpack chemistry. In: Davies, T.D., Tranter, M., Jones, H.G. (Eds.), Seasonal Snowpacks. Springer Berlin Heidelberg, pp. 115–138. https://doi.org/10.1007/978-3-642-75112-7_5.
Deocampo, D.M., 2010. Chapter 1 the geochemistry of continental carbonates. In: Developments in Sedimentology. Elsevier, pp. 1–59. https://doi.org/10.1016/S0070-4571(09)06201-3.
Donkor, K.K., Kratochvil, B., Duke, M.J.M., 1996. Estimation of the fines content of Athabasca oil sands using instrumental neutron activation analysis. Can. J. Chem. 74, 583–590. https://doi.org/10.1139/v96-062.
Dumont, M., Gascoin, S., Réveillet, M., Voisin, D., Tuzet, F., Arnaud, L., Bonnefoy, M., Bacardit Peñarroya, M., Carmagnola, C., Deguine, A., Diacre, A., Dürr, L., Evrard, O., Fontaine, F., Frankl, A., Fructus, M., Gandois, L., Gouttevin, I., Gherab, A., Hagenmuller, P., Hansson, S., Herbin, H., Josse, B., Jourdain, B., Lefevre, I., Le Roux, G., Libois, Q., Liger, L., Morin, S., Petitprez, D., Robledano, A., Schneebeli, M., Salze, P., Six, D., Thibert, E., Trachsel, J., Vernay, M., Viallon-Galinier, L., Voiron, C., 2023. Spatial variability of Saharan dust deposition revealed through a citizen science campaign. Earth Syst. Sci. Data 15, 3075–3094. https://doi.org/10.5194/essd-15-3075-2023.
Dunn, G., Bakker, K., Harris, L., 2014. Drinking water quality guidelines across Canadian provinces and territories: jurisdictional variation in the context of decentralized water governance. Int. J. Environ. Res. Publ. Health 11, 4634–4651. https://doi.org/10.3390/ijerph110504634.
Edgerton, E.S., Fort, J.M., Baumann, K., Graney, J.R., Landis, M.S., Berryman, S., Krupa, S., 2012. Method for extraction and multielement analysis of Hypogymnia physodes samples from the Athabasca Oil Sands region. In: Developments in Environmental Science. Elsevier, pp. 315–342. https://doi.org/10.1016/B978-0-08-097760-7.00014-7.
Edgerton, E.S., Hsu, Y.-M., White, E.M., Fenn, M.E., Landis, M.S., 2020. Ambient concentrations and total deposition of inorganic sulfur, inorganic nitrogen and base cations in the Athabasca Oil Sands Region. Sci. Total Environ. 706, 134864 https://doi.org/10.1016/j.scitotenv.2019.134864.
Elguero, J., Alkorta, I., 2023. The dubious origin of beryllium toxicity. Struct. Chem. 34, 391–398. https://doi.org/10.1007/s11224-023-02130-2.
EPA, 2023. United States environmental protection agency. In: National Recommended Water Quality Criteria - Aquatic Life Criteria Table.
Fassnacht, S.R., Duncan, C.R., Pfohl, A.K.D., Webb, R.W., Derry, J.E., Sanford, W.E., Reimanis, D.C., Doskocil, L.G., 2022. Drivers of dust-enhanced snowpack melt-out and streamflow timing. Hydrology 9, 47. https://doi.org/10.3390/hydrology9030047.
Feng, X., Kirchner, J.W., Renshaw, C.E., Osterhuber, R.S., Klaue, B., Taylor, S., 2001. A study of solute transport mechanisms using rare earth element tracers and artificial rainstorms on snow. Water Resour. Res. 37, 1425–1435. https://doi.org/10.1029/2000WR900376.
Field, J.P., Belnap, J., Breshears, D.D., Neff, J.C., Okin, G.S., Whicker, J.J., Painter, T.H., Ravi, S., Reheis, M.C., Reynolds, R.L., 2010. The ecology of dust. Front. Ecol. Environ. 8, 423–430. https://doi.org/10.1890/090050.
Fiera, 2013. Fiera Biological Consulting Ltd. State of the Watershed Report - Phase 3: Water Quantity and Basic Water Quality in the Athabasca Watershed. Report prepared for the Athabasca Watershed Council. Fiera Biological Consulting Report #1234.
Frisbie, S.H., Mitchell, E.J., 2022. Arsenic in drinking water: an analysis of global drinking water regulations and recommendations for updates to protect public health. PLoS One 17, e0263505. https://doi.org/10.1371/journal.pone.0263505.
Fustic, M., Nair, R., Wetzel, A., Siddiqui, R., Matthews, W., Wust, R., Bringue, M., Radovic, J., 2021. Bioturbation, heavy mineral concentration, and high gamma-ray activity in the Lower Cretaceous McMurray Formation, Canada. Palaeogeogr. Palaeoclimatol. Palaeoecol. 564, 110187 https://doi.org/10.1016/j.palaeo.2020.110187.
Gabrielli, P., Cozzi, G., Torcini, S., Cescon, P., Barbante, C., 2008. Trace elements in winter snow of the Dolomites (Italy): a statistical study of natural and anthropogenic contributions. Chemosphere 72, 1504–1509. https://doi.org/10.1016/j.chemosphere.2008.04.076.
Galarraga, C.E., Pereira-Almao, P., 2010. Hydrocracking of Athabasca Bitumen using submicronic multimetallic catalysts at near in-reservoir conditions. Energy Fuels 24, 2383–2389. https://doi.org/10.1021/ef9013407.
Ghotbizadeh, M., Cuss, C.W., Grant-Weaver, I., Markov, A., Noernberg, T., Ulrich, A., Shotyk, W., 2022. Spatiotemporal variations of total and dissolved trace elements and their distributions amongst major colloidal forms along and across the lower Athabasca River. J. Hydrol.: Reg. Stud. 40, 101029 https://doi.org/10.1016/j.ejrh.2022.101029.
Goldschmidt, V.M., 1937. The principles of distribution of chemical elements in minerals and rocks. The seventh Hugo Müller Lecture, delivered before the Chemical Society on March 17th, 1937. J. Chem. Soc. 0, 655–673. https://doi.org/10.1039/JR9370000655.
Gopalapillai, Y., Kirk, J.L., Landis, M.S., Muir, D.C.G., Cooke, C.A., Gleason, A., Ho, A., Kelly, E., Schindler, D., Wang, X., Lawson, G., 2019. Source analysis of pollutant elements in winter air deposition in the Athabasca Oil Sands Region: a temporal and spatial study. ACS Earth Space Chem. 3, 1656–1668. https://doi.org/10.1021/acsearthspacechem.9b00150.
Gosselin, P., Hrudey, M., Naeth, A., Plourde, R., Therrien, G., Van Der Kraak, Z., Xu, Z., 2010. Environmental and Health Impacts of Canada's Oil Sands Industry the Royal Society of Canada (RSC). Royal Society of Canada, Ottawa, Ontario.
Government of Alberta, 2012. Used oil as dust suppressant. Acceptable Industry Practices. https://open.alberta.ca/publications/used-oil-as-dust-suppressant-acceptable-industry-practices.
Government of Canada, 2022. Historical climate data. https://climate.weather.gc.ca/historical_data/search_historic_data_e.html.
Guéguen, C., Cuss, C.W., Cho, S., 2016. Snowpack deposition of trace elements in the Athabasca oil sands region, Canada. Chemosphere 153, 447–454. https://doi.org/10.1016/j.chemosphere.2016.03.020.
Hibberd, S., 1984. A model for pollutant concentrations during snow-melt. J. Glaciol. 30, 58–65. https://doi.org/10.3189/S0022143000008492.
Hodgson, G.W., 1954. Vanadium, nickel, and iron trace metals in crude oils of western Canada. Bulletin 38. https://doi.org/10.1306/5CEAE0C4-16BB-11D7-8645000102C1865D.
Hopke, P.K., Dai, Q., Li, L., Feng, Y., 2020. Global review of recent source apportionments for airborne particulate matter. Sci. Total Environ. 740, 140091 https://doi.org/10.1016/j.scitotenv.2020.140091.
Jang, H., Etsell, T.H., 2005. Morphological and mineralogical characterization of oil sands fly ash. Energy Fuels 19, 2121–2128. https://doi.org/10.1021/ef050123a.
Javed, M.B., Cuss, C.W., Grant-Weaver, I., Shotyk, W., 2017. Size-resolved Pb distribution in the Athabasca River shows snowmelt in the bituminous sands region an insignificant source of dissolved Pb. Sci. Rep. 7, 43622 https://doi.org/10.1038/srep43622.
Javed, M.B., Cuss, C.W., Zheng, J., Grant-Weaver, I., Noernberg, T., Shotyk, W., 2022. Size-fractionation of trace elements in dusty snow from open pit bitumen mines and upgraders: collection, handling, preparation and analysis of samples from the Athabasca Bituminous Sands region of Alberta, Canada. Environ. Sci.: Atmos. https://doi.org/10.1039/D1EA00034A, 10.1039.D1EA00034A.
Javed, M.B., Grant-Weaver, I., Shotyk, W., 2020. An optimized HNO3 and HBF4 digestion method for multielemental soil and sediment analysis using inductively coupled plasma quadrupole mass spectrometry. Can. J. Soil Sci. 100, 393–407. https://doi.org/10.1139/cjss-2020-0001.
Javed, M.B., Shotyk, W., 2018. Estimating bioaccessibility of trace elements in particles suspended in the Athabasca River using sequential extraction. Environ. Pollut. 240, 466–474. https://doi.org/10.1016/j.envpol.2018.04.131.
Johannessen, M., Henriksen, A., 1978. Chemistry of snow meltwater: changes in concentration during melting. Water Resour. Res. 14, 615–619. https://doi.org/10.1029/WR014i004p00615.
Kaminsky, H., Etsell, T., Ivey, D.G., Omotoso, O., 2006. Fundamental particle size of clay minerals in Athabasca Oil Sands tailings. https://doi.org/10.11362/jcssjclayscience1960.12.Supplement2_217.
Kaminsky, H.A.W., Etsell, T.H., Ivey, D.G., Omotoso, O., 2008. Characterization of heavy minerals in the Athabasca oil sands. Miner. Eng. 21, 264–271. https://doi.org/10.1016/j.mineng.2007.09.011.
Kelly, E.N., Schindler, D.W., Hodson, P.V., Short, J.W., Radmanovich, R., Nielsen, C.C., 2010. Oil sands development contributes elements toxic at low concentrations to the Athabasca River and its tributaries. Proc. Natl. Acad. Sci. USA 107, 16178–16183. https://doi.org/10.1073/pnas.1008754107.
Kirk, J., Muir, D., Manzano, C., Cooke, C., Wiklund, J., Gleason, A., Summers, J., Smol, J., Kurek, J., 2018. Atmospheric deposition to the Athabasca Oil Sands Region using snowpack measurements and dated lake sediment cores. Oil Sands Monitoring Program Technical Report 43. Series No. 1.2.
Koffman, B.G., Handley, M.J., Osterberg, E.C., Wells, M.L., Kreutz, K.J., 2014. Dependence of ice-core relative trace-element concentration on acidification. J. Glaciol. 60, 103–112. https://doi.org/10.3189/2014JoG13J137.
Kok, J.F., Storelvmo, T., Karydis, V.A., Adebiyi, A.A., Mahowald, N.M., Evan, A.T., He, C., Leung, D.M., 2023. Mineral dust aerosol impacts on global climate and climate change. Nat. Rev. Earth Environ. 4, 71–86. https://doi.org/10.1038/s43017-022-00379-5.
Krachler, M., Zheng, J., Fisher, D., Shotyk, W., 2005a. Analytical procedures for improved trace element detection limits in polar ice from Arctic Canada using ICP-SMS. Anal. Chim. Acta 530, 291–298. https://doi.org/10.1016/j.aca.2004.09.024.
Krachler, M., Zheng, J., Koerner, R., Zdanowicz, C., Fisher, D., Shotyk, W., 2005b. Increasing atmospheric antimony contamination in the northern hemisphere: snow and ice evidence from Devon Island, Arctic Canada. J. Environ. Monit. 7, 1169. https://doi.org/10.1039/b509373b.
Lai, A.M., Shafer, M.M., Dibb, J.E., Polashenski, C.M., Schauer, J.J., 2017. Elements and inorganic ions as source tracers in recent Greenland snow. Atmos. Environ. 164, 205–215. https://doi.org/10.1016/j.atmosenv.2017.05.048.
Landis, M.S., Pancras, J.P., Graney, J.R., Stevens, R.K., Percy, K.E., Krupa, S., 2012. Receptor modeling of epiphytic lichens to elucidate the sources and spatial distribution of inorganic air pollution in the Athabasca Oil Sands region. In:

Developments in Environmental Science. Elsevier, pp. 427–467. https://doi.org/10.1016/B978-0-08-097760-7.00018-4.
Landis, M.S., Patrick Pancras, J., Graney, J.R., White, E.M., Edgerton, E.S., Legge, A., Percy, K.E., 2017. Source apportionment of ambient fine and coarse particulate matter at the Fort McKay community site, in the Athabasca Oil Sands Region, Alberta, Canada. Sci. Total Environ. 584–585, 105–117. https://doi.org/10.1016/j.scitotenv.2017.01.110.
Lawrence, C.R., Painter, T.H., Landry, C.C., Neff, J.C., 2010. Contemporary geochemical composition and flux of aeolian dust to the San Juan Mountains, Colorado, United States. J. Geophys. Res. 115, G03007 https://doi.org/10.1029/2009JG001077.
Lee, J., Jung, H., 2022. Understanding the relationship between meltwater discharge and solute concentration by modeling solute transport in a snowpack in snow-dominated regions – a review. Polar Science 31, 100782. https://doi.org/10.1016/j.polar.2021.100782.
Lehning, M., 2005. Energy balance and thermophysical processes in snowpacks. In: Anderson, M.G., McDonnell, J.J. (Eds.), Encyclopedia of Hydrological Sciences. John Wiley & Sons, Ltd, Chichester, UK, p. hsa166. https://doi.org/10.1002/0470848944.hsa166.
Lenth, R.V., 2016. Least-squares means: the R Package lsmeans. J. Stat. Software 69. https://doi.org/10.18637/jss.v069.i01.
Li, L., Zhang, R., Li, Q., Zhang, K., Liu, Z., Ren, Z., 2023. Multidimensional spatial monitoring of open pit mine dust dispersion by unmanned aerial vehicle. Sci. Rep. 13, 6815. https://doi.org/10.1038/s41598-023-33714-x.
Li, Y., Li, Z., Cozzi, G., Turetta, C., Barbante, C., Huang, J., Xiong, L., 2018. Signals of pollution revealed by trace elements in recent snow from mountain glaciers at the Qinghai–Tibetan plateau. Chemosphere 200, 523–531. https://doi.org/10.1016/j.chemosphere.2018.01.039.
Luo, X., Bing, H., Luo, Z., Wang, Y., Jin, L., 2019. Impacts of atmospheric particulate matter pollution on environmental biogeochemistry of trace metals in soil-plant system: a review. Environ. Pollut. 255, 113138 https://doi.org/10.1016/j.envpol.2019.113138.
Lynam, M.M., Dvonch, J.T., Barres, J.A., Morishita, M., Legge, A., Percy, K., 2015. Oil sands development and its impact on atmospheric wet deposition of air pollutants to the Athabasca Oil Sands Region, Alberta, Canada. Environ. Pollut. 206, 469–478. https://doi.org/10.1016/j.envpol.2015.07.032.
Mamun, A.A., Celo, V., Dabek-Zlotorzynska, E., Charland, J.-P., Cheng, I., Zhang, L., 2021. Characterization and source apportionment of airborne particulate elements in the Athabasca oil sands region. Sci. Total Environ. 788, 147748 https://doi.org/10.1016/j.scitotenv.2021.147748.
Mamun, A.A., Cheng, I., Zhang, L., Celo, V., Dabek-Zlotorzynska, E., Charland, J., 2022. Estimation of atmospheric dry and wet deposition of particulate elements at four monitoring sites in the Canadian Athabasca oil sands region. J. Geophys. Res. Atmos. 127 https://doi.org/10.1029/2021JD035787.
Masau, M., Cerny, P., Chapman, R., 2000. Exsolution of zirconian-hafnian wodginite from manganoan-tantalian cassiterite, annie claim #3 granitic pegmatite, southeastern manitoba, Canada. Can. Mineral. 38, 685–694. https://doi.org/10.2113/gscanmin.38.3.685.
Mellon, G.B., 1956. Geology of the McMurray Formation. Part II. Heavy Minerals of the McMurray Formation, vol. 72. Research Council of Alberta, Edmonton, Alberta, Canada, pp. 30–43. Report.
Möller, P., De Lucia, M., 2020. Incorporation of rare earths and yttrium in calcite: a critical Re-evaluation. Aquat. Geochem. 26, 89–117. https://doi.org/10.1007/s10498-020-09369-9.
Morman, S.A., Plumlee, G.S., 2013. The role of airborne mineral dusts in human disease. Aeolian Res. 9, 203–212. https://doi.org/10.1016/j.aeolia.2012.12.001.
Mossop, G.D., 1980. Geology of the Athabasca oil sands. Science 207, 145–152. https://doi.org/10.1126/science.207.4427.145.
Murray, W.A., 1981. The 1981 Snowpack Survey in the AOSERP Study Area. University of Alberta Libraries. https://doi.org/10.7939/R3H41JQ66.
Nesbitt, J.A., Lindsay, M.B.J., 2017. Vanadium geochemistry of oil sands fluid petroleum coke. Environ. Sci. Technol. 51, 3102–3109. https://doi.org/10.1021/acs.est.6b05682.
Nesbitt, J.A., Lindsay, M.B.J., Chen, N., 2017. Geochemical characteristics of oil sands fluid petroleum coke. Appl. Geochem. 76, 148–158. https://doi.org/10.1016/j.apgeochem.2016.11.023.
Osacky, M., Geramian, M., Ivey, D.G., Liu, Q., Etsell, T.H., 2013. Mineralogical and chemical composition of petrologic end members of Alberta oil sands. Fuel 113, 148–157. https://doi.org/10.1016/j.fuel.2013.05.099.
Pačes, T., Krachler, M., Novák, M., Štěpánová, M., Bohdálková, L., Přechová, E., 2023. Atmospheric deposition and trajectories of antimony in Central Europe. Environ. Pollut. 316, 120518 https://doi.org/10.1016/j.envpol.2022.120518.
Panta, A., Kandler, K., Alastuey, A., González-Flórez, C., González-Romero, A., Klose, M., Querol, X., Reche, C., Yus-Díez, J., Pérez García-Pando, C., 2023. Insights into the single-particle composition, size, mixing state, and aspect ratio of freshly emitted mineral dust from field measurements in the Moroccan Sahara using electron microscopy. Atmos. Chem. Phys. 23, 3861–3885. https://doi.org/10.5194/acp-23-3861-2023.
Pawlas, N., Pałczyński, C.M., 2022. Beryllium. In: Handbook on the Toxicology of Metals. Elsevier, pp. 101–119. https://doi.org/10.1016/B978-0-12-822946-0.00004-0.
Pekov, I.V., Zubkova, N.V., Chukanov, N.V., Agakhanov, A.A., Belakovskiy, D.I., Horvath, L., Filinchuk, Y.E., Gobechiya, E.R., Pushcharovsky, D.Yu, Rabadanov, M. Kh, 2008. Niveolanite, the first natural beryllium carbonate, a new mineral species from Mont Saint Hilaire, Quebec, Canada. Can. Mineral. 46, 1343–1354. https://doi.org/10.3749/canmin.46.5.1343.
Pey, J., Revuelto, J., Moreno, N., Alonso-González, E., Bartolomé, M., Reyes, J., Gascoin, S., López-Moreno, J.I., 2020. Snow impurities in the Central Pyrenees: from their geochemical and mineralogical composition towards their impacts on snow albedo. Atmosphere 11, 937. https://doi.org/10.3390/atmos11090937.
Phillips, C.R., Chao, K.S., 1977. Desulphurization of Athabasca petroleum coke by (a) chemical oxidation and (b) solvent extraction. Fuel 56, 70–72. https://doi.org/10.1016/0016-2361(77)90045-X.
Pu, W., Cui, J., Wu, D., Shi, T., Chen, Y., Xing, Y., Zhou, Y., Wang, X., 2021. Unprecedented snow darkening and melting in New Zealand due to 2019–2020 Australian wildfires. Fundam. Res. 1, 224–231. https://doi.org/10.1016/j.fmre.2021.04.001.
R Core Team, 2021. R: a language and environment for statistical computing. URL. https://www.R-project.org/.
Rember, R.D., Trefry, J.H., 2004. Increased concentrations of dissolved trace metals and organic carbon during snowmelt in rivers of the Alaskan Arctic. Geochem. Cosmochim. Acta 68, 477–489. https://doi.org/10.1016/S0016-7037(03)00458-7.
Reynolds, R.L., Goldstein, H.L., Moskowitz, B.M., Kokaly, R.F., Munson, S.M., Solheid, P., Breit, G.N., Lawrence, C.R., Derry, J., 2020. Dust deposited on snow cover in the San Juan Mountains, Colorado, 2011–2016: compositional variability bearing on snowmelt effects. J. Geophys. Res. Atmos. 125 https://doi.org/10.1029/2019JD032210.
Rhoades, C., Elder, K., Greene, E., 2010. The Influence of an extensive dust event on snow chemistry in the southern Rocky Mountains. Arctic Antarct. Alpine Res. 42, 98–105. https://doi.org/10.1657/1938-4246-42.1.98.
Robertson, J.M., Nesbitt, J.A., Lindsay, M.B.J., 2019. Aqueous- and solid-phase molybdenum geochemistry of oil sands fluid petroleum coke deposits, Alberta, Canada. Chemosphere 217, 715–723. https://doi.org/10.1016/j.chemosphere.2018.11.064.
Rodríguez, S., Alastuey, A., Querol, X., 2012. A review of methods for long term in situ characterization of aerosol dust. Aeolian Res. 6, 55–74. https://doi.org/10.1016/j.aeolia.2012.07.004.
Roth, E., Bank, T., Howard, B., Granite, E., 2017. Rare earth elements in Alberta oil sand process streams. Energy Fuels 31, 4714–4720. https://doi.org/10.1021/acs.energyfuels.6b03184.
Rudnick, R.L., Gao, S., 2014. Composition of the continental crust. In: Treatise on Geochemistry. Elsevier, pp. 1–51. https://doi.org/10.1016/B978-0-08-095975-7.00301-6.
Schepanski, K., 2018. Transport of mineral dust and its impact on climate. Geosciences 8, 151. https://doi.org/10.3390/geosciences8050151.
Scheuvens, D., Kandler, K., 2014. On composition, morphology, and size distribution of airborne mineral dust. In: Knippertz, P., Stuut, J.-B.W. (Eds.), Mineral Dust. Springer, Netherlands, Dordrecht, pp. 15–49. https://doi.org/10.1007/978-94-017-8978-3_2.
Seinfeld, J.H., Pandis, S.N., 2016. Atmospheric Chemistry and Physics: from Air Pollution to Climate Change, third ed. John Wiley & Sons, Hoboken, New Jersey.
Shahzad, B., Mughal, M.N., Tanveer, M., Gupta, D., Abbas, G., 2017. Is lithium biologically an important or toxic element to living organisms? An overview. Environ. Sci. Pollut. Res. 24, 103–115. https://doi.org/10.1007/s11356-016-7898-0.
Wind erosion and wind-erosion research. In: Shao, Y. (Ed.), 2009. Physics and Modelling of Wind Erosion, Atmospheric and Oceanographic Sciences Library. Springer, Netherlands, Dordrecht, pp. 1–11. https://doi.org/10.1007/978-1-4020-8895-7_1.
Shotyk, W., Belland, R., Duke, J., Kempter, H., Krachler, M., Noernberg, T., Pelletier, R., Vile, M.A., Wieder, K., Zaccone, C., Zhang, S., 2014. Sphagnum mosses from 21 ombrotrophic bogs in the Athabasca Bituminous Sands Region show no significant atmospheric contamination of "heavy metals.". Environ. Sci. Technol. 48, 12603–12611. https://doi.org/10.1021/es503751v.
Shotyk, W., Bicalho, B., Cuss, C.W., Duke, M.J.M., Noernberg, T., Pelletier, R., Steinnes, E., Zaccone, C., 2016. Dust is the dominant source of "heavy metals" to peat moss (Sphagnum fuscum) in the bogs of the Athabasca Bituminous Sands region of northern Alberta. Environ. Int. 92–93, 494–506. https://doi.org/10.1016/j.envint.2016.03.018.
Shotyk, W., Appleby, P.G., Bicalho, B., Davies, L.J., Froese, D., Grant-Weaver, I., Magnan, G., Mullan-Boudreau, G., Noernberg, T., Pelletier, R., Shannon, B., van Bellen, S., Zaccone, C., 2017a. Peat bogs document decades of declining atmospheric contamination by trace metals in the Athabasca bituminous sands region. Environ. Sci. Technol. 51, 6237–6249. https://doi.org/10.1021/acs.est.6b04909.
Shotyk, W., Bicalho, B., Cuss, C.W., Donner, M.W., Grant-Weaver, I., Haas-Neill, S., Javed, M.B., Krachler, M., Noernberg, T., Pelletier, R., Zaccone, C., 2017b. Trace metals in the dissolved fraction (< 0.45 μm) of the lower Athabasca River: analytical challenges and environmental implications. Sci. Total Environ. 580, 660–669. https://doi.org/10.1016/j.scitotenv.2016.12.012.
Shotyk, W., 2020. Trace elements in wild berries from reclaimed lands: biomonitors of contamination by atmospheric dust. Ecol. Indicat. 110, 105960 https://doi.org/10.1016/j.ecolind.2019.105960.
Shotyk, W., 2022. Environmental significance of trace elements in the Athabasca Bituminous Sands: facts and misconceptions. Environ. Sci.: Process. Impacts 10, 1039. https://doi.org/10.1039/D2EM00049K. D2EM00049K.
Shotyk, W., Barraza, F., Butt, S., Chen, N., Cuss, C.W., Devito, K., Frost, L., Grant-Weaver, I., Javed, M.B., Noernberg, T., Oleksandrenko, A., 2023. Trace elements in peat bog porewaters: indicators of dissolution of atmospheric dusts and aerosols from anthropogenic and natural sources. Environ. Sci.: Water Res. Technol. 10 https://doi.org/10.1039/D3EW00241A, 1039.D3EW00241A.
Šidák, Z., 1967. Rectangular confidence regions for the means of multivariate normal distributions. J. Am. Stat. Assoc. 62, 626–633. https://doi.org/10.1080/01621459.1967.10482935.
Simon, D.E., Anderson, M.S., 1990. Stability of clay minerals in acid. In: All Days. Presented at the SPE Formation Damage Control Symposium, SPE. Lafayette, Louisiana. https://doi.org/10.2118/19422-MS. SPE-19422-MS.

Simonson, R.W., 1995. Airborne dust and its significance to soils. Geoderma 65, 1–43. https://doi.org/10.1016/0016-7061(94)00031-5.
Smrzka, D., Zwicker, J., Bach, W., Feng, D., Himmler, T., Chen, D., Peckmann, J., 2019. The behavior of trace elements in seawater, sedimentary pore water, and their incorporation into carbonate minerals: a review. Facies 65, 41. https://doi.org/10.1007/s10347-019-0581-4.
Spiers, G.A., Dudas, M.J., Turchenek, L.W., 1989. The chemical and mineralogical composition of soil parent materials in northeast Alberta. Can. J. Soil Sci. 69, 721–737. https://doi.org/10.4141/cjss89-074.
Spolaor, A., Moroni, B., Luks, B., Nawrot, A., Roman, M., Larose, C., Stachnik, Ł., Bruschi, F., Kozioł, K., Pawlak, F., Turetta, C., Barbaro, E., Gallet, J.-C., Cappelletti, D., 2021. Investigation on the sources and impact of trace elements in the annual snowpack and the firn in the Hansbreen (southwest Spitsbergen). Front in Earth Sci. 8, 536036 https://doi.org/10.3389/feart.2020.536036.
Stachiw, S., Bicalho, B., Grant-Weaver, I., Noernberg, T., Shotyk, W., 2019. Trace elements in berries collected near upgraders and open pit mines in the Athabasca Bituminous Sands Region (ABSR): distinguishing atmospheric dust deposition from plant uptake. Sci. Total Environ. 670, 849–864. https://doi.org/10.1016/j.scitotenv.2019.03.238.
Starkey, H., 1982. The Role of Clays in Fixing Lithium. USGS. https://doi.org/10.3133/b1278F.
Stearney, E.R., Jakubowski, J.A., Regina, A.C., 2023. Beryllium toxicity. In: StatPearls. StatPearls Publishing, Treasure Island (FL).
Svensson, J., Ström, J., Honkanen, H., Asmi, E., Dkhar, N.B., Tayal, S., Sharma, V.P., Hooda, R., Leppäranta, M., Jacobi, H.-W., Lihavainen, H., Hyvärinen, A., 2021. Deposition of light-absorbing particles in glacier snow of the Sunderdhunga Valley, the southern forefront of the central Himalayas. Atmos. Chem. Phys. 21, 2931–2943. https://doi.org/10.5194/acp-21-2931-2021.
Tadesse, B., Makuei, F., Albijanic, B., Dyer, L., 2019. The beneficiation of lithium minerals from hard rock ores: a review. Miner. Eng. 131, 170–184. https://doi.org/10.1016/j.mineng.2018.11.023.
Taylor, T.P., Ding, M., Ehler, D.S., Foreman, T.M., Kaszuba, J.P., Sauer, N.N., 2003. Beryllium in the environment: a review. J. Environ. Sci. Health, Part A 38, 439–469. https://doi.org/10.1081/ESE-120016906.
The European Comission, 2013. Directive 2013/39/EU of the European Parliament and of the Council of 12 August 2013 Amending Directives 2000/60/EC and 2008/105/EC as Regards Priority Substances in the Field of Water Policy Text with EEA Relevance.
Tuzet, F., Dumont, M., Lafaysse, M., Picard, G., Arnaud, L., Voisin, D., Lejeune, Y., Charrois, L., Nabat, P., Morin, S., 2017. A multilayer physically based snowpack model simulating direct and indirect radiative impacts of light-absorbing impurities in snow. Cryosphere 11, 2633–2653. https://doi.org/10.5194/tc-11-2633-2017.
Tylenda, C.A., Tomei Torres, F.A., Sullivan, D.W., 2022. Antimony. In: Handbook on the Toxicology of Metals. Elsevier, pp. 23–40. https://doi.org/10.1016/B978-0-12-822946-0.00002-7.
Vesely, J., Norton, S.A., Skrivan, P., Majer, V., Kram, P., Navratil, T., Kaste, J.M., 2002. Environmental chemistry of beryllium. Rev. Mineral. Geochem. 50, 291–317. https://doi.org/10.2138/rmg.2002.50.7.
Vithanage, M., Bandara, P.C., Novo, L.A.B., Kumar, A., Ambade, B., Naveendrakumar, G., Ranagalage, M., Magana-Arachchi, D.N., 2022. Deposition of trace metals associated with atmospheric particulate matter: environmental fate and health risk assessment. Chemosphere 303, 135051. https://doi.org/10.1016/j.chemosphere.2022.135051.
Wang, L., Putnis, C.V., 2020. Dissolution and precipitation dynamics at environmental mineral interfaces imaged by in situ atomic force microscopy. Account. Chem. Res. 53, 1196–1205. https://doi.org/10.1021/acs.accounts.0c00128.
Wang, X., Chow, J.C., Kohl, S.D., Yatavelli, L.N.R., Percy, K.E., Legge, A.H., Watson, J.G., 2015. Wind erosion potential for fugitive dust sources in the Athabasca Oil Sands Region. Aeolian Res. 18, 121–134. https://doi.org/10.1016/j.aeolia.2015.07.004.
Wang, Z.-M., Zhou, W., Jiskani, I.M., Ding, X.-H., Liu, Z.-C., Qiao, Y.-Z., Luan, B., 2021. Dust reduction method based on water infusion blasting in open-pit mines: a step toward green mining. Energy Sources, Part A Recovery, Util. Environ. Eff. 1–15. https://doi.org/10.1080/15567036.2021.1903118.
Warren, S.G., 2019. Light-absorbing impurities in snow: a personal and historical account. Front. Earth Sci. 6, 250. https://doi.org/10.3389/feart.2018.00250.
Wiklund, J.A., Kirk, J.L., Muir, D.C.G., Gleason, A., Carrier, J., Yang, F., 2020. Atmospheric trace metal deposition to remote Northwest Ontario, Canada: anthropogenic fluxes and inventories from 1860 to 2010. Sci. Total Environ. 749, 142276 https://doi.org/10.1016/j.scitotenv.2020.142276.
Xing, Z., Du, K., 2017. Particulate matter emissions over the oil sands regions in Alberta, Canada. Environ. Rev. 25, 432–443. https://doi.org/10.1139/er-2016-0112.
Yang, F., Mamun, A.A., Cheng, I., Qiu, X., Zhang, L., 2023. Contributions of the oil sands sources to the ambient concentrations and deposition of particulate elements in the Canadian Athabasca oil sands region. Sci. Total Environ. 898, 165519 https://doi.org/10.1016/j.scitotenv.2023.165519.
Zhang, X., Guo, J., Wu, S., Chen, F., Yang, Y., 2020. Divalent heavy metals and uranyl cations incorporated in calcite change its dissolution process. Sci. Rep. 10, 16864 https://doi.org/10.1038/s41598-020-73555-6.
Zhang, Y., Shotyk, W., Zaccone, C., Noernberg, T., Pelletier, R., Bicalho, B., Froese, D.G., Davies, L., Martin, J.W., 2016. Airborne petcoke dust is a major source of polycyclic aromatic hydrocarbons in the Athabasca Oil Sands Region. Environ. Sci. Technol. 50, 1711–1720. https://doi.org/10.1021/acs.est.5b05092.
Zhao, F., Liu, Y., Lu, N., Xu, T., Zhu, G., Wang, K., 2021. A review on upgrading and viscosity reduction of heavy oil and bitumen by underground catalytic cracking. Energy Rep. 7, 4249–4272. https://doi.org/10.1016/j.egyr.2021.06.094.
Zuliani, J.E., Miyata, T., Mizoguchi, T., Feng, J., Kirk, D.W., Jia, C.Q., 2016. Characterization of vanadium in oil sands fluid petroleum coke using electron microscopy. Fuel 178, 124–128. https://doi.org/10.1016/j.fuel.2016.03.015.